

Review

# Lipase Immobilization in Mesoporous Silica Nanoparticles for Biofuel Production

Aniello Costantini <sup>1,\*</sup> and Valeria Califano <sup>2,\*</sup>

<sup>1</sup> Department of Chemical Engineering, Materials and Industrial Production, Università degli Studi di Napoli Federico II, P.le Tecchio 80, 80125 Napoli, Italy

<sup>2</sup> Institute of Sciences and Technologies for Sustainable Energy and Mobility (STEMS), Italian National Research Council, Via G. Marconi 4, 80125 Napoli, Italy

\* Correspondence: anicosta@unina.it (A.C.); valeria.califano@stems.cnr.it (V.C.)

**Abstract:** Lipases are ubiquitous enzymes whose physiological role is the hydrolysis of triacylglycerol into fatty acids. They are the most studied and industrially interesting enzymes, thanks to their versatility to promote a plethora of reactions on a wide range of substrates. In fact, depending on the reaction conditions, they can also catalyze synthesis reactions, such as esterification, acidolysis and transesterification. The latter is particularly important for biodiesel production. Biodiesel can be produced from animal fats or vegetable oils and is considered as a biodegradable, non-toxic and renewable energy source. The use of lipases as industrial catalysts is subordinated to their immobilization on insoluble supports, to allow multiple uses and use in continuous processes, but also to stabilize the enzyme, intrinsically prone to denaturation with consequent loss of activity. Among the materials that can be used for lipase immobilization, mesoporous silica nanoparticles represent a good choice due to the combination of thermal and mechanical stability with controlled textural characteristics. Moreover, the presence of abundant surface hydroxyl groups allows for easy chemical surface functionalization. This latter aspect has the main importance since lipases have a high affinity with hydrophobic supports. The objective of this work is to provide an overview of the recent progress of lipase immobilization in mesoporous silica nanoparticles with a focus on biodiesel production.

**Keywords:** lipase; enzyme immobilization; mesoporous silica



**Citation:** Costantini, A.; Califano, V. Lipase Immobilization in Mesoporous Silica Nanoparticles for Biofuel Production. *Catalysts* **2021**, *11*, 629. <https://doi.org/10.3390/catal11050629>

Academic Editor:

Roberto Fernandez-Lafuente

Received: 24 April 2021

Accepted: 11 May 2021

Published: 13 May 2021

**Publisher's Note:** MDPI stays neutral with regard to jurisdictional claims in published maps and institutional affiliations.



**Copyright:** © 2021 by the authors. Licensee MDPI, Basel, Switzerland. This article is an open access article distributed under the terms and conditions of the Creative Commons Attribution (CC BY) license (<https://creativecommons.org/licenses/by/4.0/>).

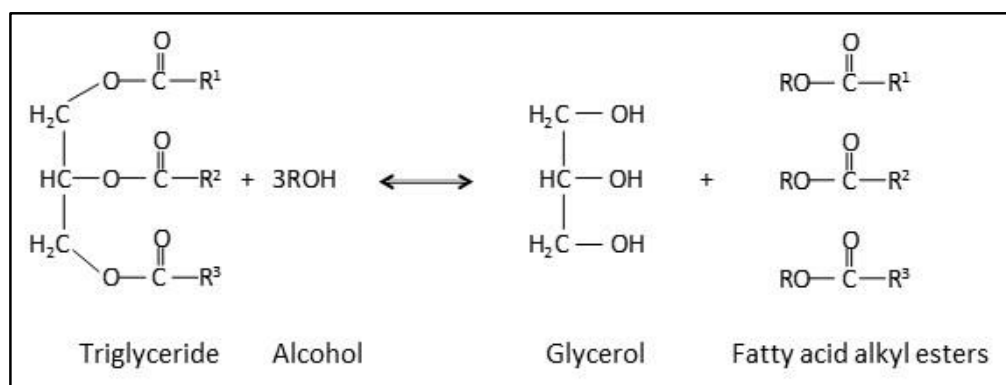
## 1. Introduction

Lipases (triacylglycerol ester hydrolases, EC 3.1.1.3) are ubiquitous enzymes that can be found in animals, plants and natural or genetically engineered microorganisms. Physiologically, they play a key role in fat digestion by catalyzing the hydrolysis of fats and oils, releasing free fatty acids, diacylglycerols, monoglycerols and glycerol. Lipases catalyze reactions of water-insoluble substrates and the presence of the water/lipid interface is a usual prerequisite for efficient catalysis [1]. Besides this, depending on the water content of the reaction environment, they can promote synthesis reactions, such as esterification [2], transesterification [3] and acidolysis [4]. These reactions can take place in organic solvents.

Due to their great versatility, lipases are recognized as the most important group of catalysts in biotechnology [5]. They find use in a variety of biotechnological fields such as food and dairy, pharmaceutical, agrochemical, oleochemical, cosmetic industries and detergents [6,7]. In particular, the enzymatic transesterification of vegetable oil and animal fat into biodiesel represents a very active research field in recent years, thanks to the benefits that biofuels can bring in the current scenario of environmental degradation. Biodiesel can attenuate the climate change concerns because it reduces the overall life-cycle of carbon dioxide emission, being produced from renewable sources. Other inherent emission reductions are hydrocarbons, carbon monoxide and particulate matter. Furthermore, it can be used in existing engines, pure or in blends, without technical modification [8].

Biodiesel can be produced from renewable sources available worldwide, addressing the problems associated with the depletion of fossil resources and political instability in oil-producing countries.

Chemically, biodiesel consists of mono-alkyl esters of fatty acids. The enzymatic transesterification of triglycerides to biodiesel proceeds stepwise in three reversible reactions. The triglyceride is converted stepwise to diglyceride, monoglyceride and finally glycerol. In each of the steps, a molecule of fatty acid ester is released. The final products are alkyl esters and glycerol (see Scheme 1).



**Scheme 1.** The transesterification reaction of triglycerides into fatty acid alkyl esters and glycerol.

The conventional method for producing biodiesel involves acid or base catalysts. The enzymatic catalysis enables milder process conditions (temperature, pressure and pH) and lower amounts of by-products, reducing environmental problems and downstream processing costs [9]. Furthermore, lipases allow treating raw materials with high content of free fatty acids, enabling the use of low-quality inedible oil and waste cooking oil [10]. However, in order for the process to be economically viable on an industrial level, it is necessary to solve two problems related to the use of enzymes: their high cost and their inherent instability. Hence the need to immobilize lipase on water-insoluble supports. Enzyme immobilization allows the development of continuous processes, an easier separation of products and the reuse of the catalyst. For lipase, the enhancement of its stability and catalytic activity was often observed upon immobilization [11–13]. Among the supports used for the immobilization of lipase, mesoporous silica materials play a prominent role [14]. Mesoporous silica represents a broad platform for enzyme immobilization, due to an easy modulation of the size, morphology and distribution of the pores by changing the synthesis parameters, and their chemical and thermal stability [15]. Moreover, the abundant surface hydroxyl groups enable easy chemical surface functionalization. This is particularly important for the immobilization of lipases. They are unique enzymes in that most of them require interfacial activation for full catalytic performance. Lipases have a helical loop that covers their active site. Upon adsorption at a hydrophobic/hydrophilic interface, the loop undergoes a conformational change from the inactive “closed” form in which the catalytic site is inaccessible to the “open” active form. It is preferable to immobilize lipase in the “open-lid” active conformation. This is possible by using hydrophobic supports, since lipases recognize hydrophobic surfaces similar to those of their natural substrates and they undergo interfacial activation during immobilization [12,16]. A hydrophobic support for adsorption can be obtained by functionalizing silica with hydrophobic groups.

The objective of this work is to provide an overview of lipase immobilization on mesoporous silica nano/microparticles and the functionalization thereof to obtain a suitable biocatalyst for biofuel production. Lipase is one of the most studied enzymes. Due to the very large number of publications on lipase immobilization [17], it is important to have sectorial reviews on specific topics to keep the state-of-the-art up to date.

## 2. Lipases

### 2.1. Three-Dimensional Structure

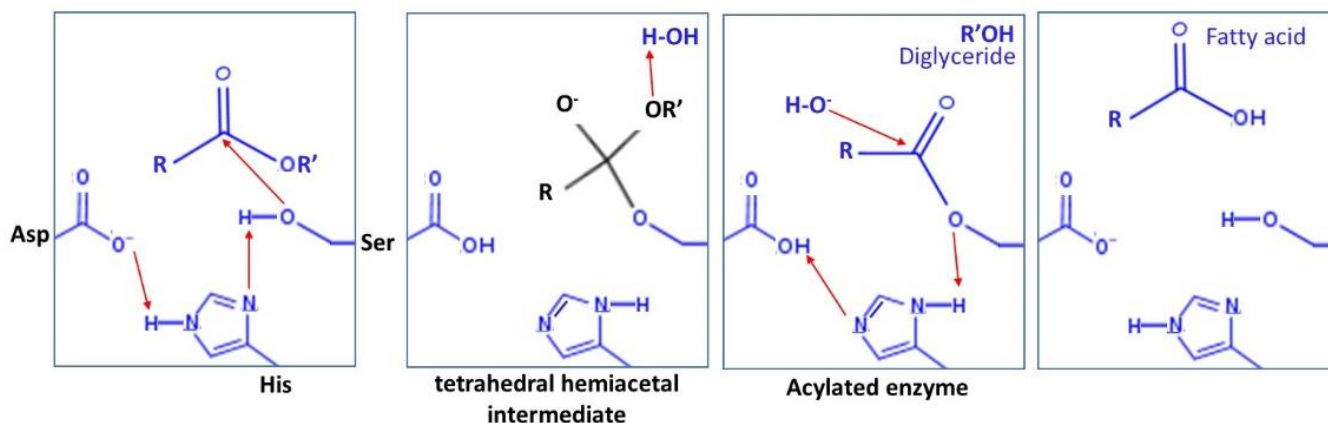
Lipases derived from animal, bacterial and fungal sources all tend to have similar three-dimensional structures. Molecular weight of lipases from different sources shows great variation but generally, they range between 20 and 60 kDa. Despite differences in size and sequence homology, most lipases adopt a similar core topology. The three-dimensional structure of *Candida rugosa* lipase (CRL) is shown in Figure 1. The characteristic pattern of lipases is a structural motif, the so-called lipase fold, which is a subset of the  $\alpha/\beta$ -hydrolase [1]. This fold comprises a central, mostly parallel  $\beta$ -sheet (in light blue in Figure 1) with several helices on both sides of the sheet (in dark green in Figure 1). The central  $\beta$ -sheet contains the catalytic residues (in red in Figure 1). In general, the polypeptide chain of lipase is folded into two domains, the C-terminal domain and the N-terminal domain. The N-terminal domain contains the active site in a hydrophobic tunnel going from the catalytic site to the surface that can accommodate a long fatty acid chain. This tunnel generally is not straight, showing an L-shape that fits with the sterical requirements of the oleic acid [18]. The active sites of lipases are composed of Ser-Glu (or Asp)-His residues (nucleophile-acid-histidine), forming a catalytic triad whose topology is highly conserved among the lipases. The residues of the catalytic triad are located at the top of the  $\beta$ -sheet near its center. The serine residue turns up a short loop between an  $\alpha$ -helix and a  $\beta$ -strand, the so-called nucleophilic elbow [19], which is well-conserved in lipases.



**Figure 1.** Ribbon diagram of CRL with open and closed states of the lid superimposed. The central mixed  $\beta$ -sheet is light blue, and the smaller N-terminal  $\beta$ -sheet is dark blue. Helices that pack against the central  $\beta$ -sheet are dark green. The closed conformation of the lid is yellow, and the open conformation is red. The residues forming the catalytic triad are shown in red [1]. Reprinted with permission: License Number: 5056440201560, license date: 26 April 2021 Elsevier, *Biochimica et Biophysica Acta (BBA)—Molecular and Cell Biology of Lipids*.

## 2.2. Mechanism of Catalysis

The catalytic mechanism for triglyceride hydrolysis is illustrated in Scheme 2. In the first step, serine is activated by deprotonation assisted by histidine and aspartate. The nucleophile oxygen of deprotonated Ser attacks the carbonyl group of the substrate, forming a tetrahedral hemiacetal intermediate with the triglyceride. In the second step, the ester bond of the hemiacetal is hydrolyzed and the diacylglyceride is released. In the third step, a nucleophile (e.g.,  $\text{OH}^-$ ) attacks the acylated enzyme, leading to a product (long-chain fatty acid) release and regeneration of the catalytic site [20].



**Scheme 2.** Mechanism of triglyceride hydrolysis catalyzed by lipase.

## 2.3. Interfacial Activation

Lipases are interfacial enzymes, i.e., they require an interface to exert their catalytic activity. This is because their physiological environment is aqueous, whereas their substrate, i.e., triglycerides, is insoluble in water. Therefore, lipase works at the water/oil interface. In aqueous solution, lipases have very low activity toward molecularly dissolved substrates, but when the substrate concentration is high enough to form micellar solutions or emulsions, i.e., interfaces, the activity of lipases is highly increased.

Most lipases possess an amphiphilic polypeptide loop, called lid or flap, covering the active site of the enzyme in aqueous environment. The lid generally contains a  $\alpha$ -helix. In the so-called 'closed state', the loop (in yellow in Figure 1) extends over the active site and makes it inaccessible to substrates. However, in the presence of a hydrophobic interface, the loop moves to the side, leading to the 'open state' conformation (in red in Figure 1). This phenomenon is known as interfacial activation and leads to the active form of the enzyme. The conformational rearrangement involves only the lid, which does not move as a rigid body but undergoes an internal rearrangement. In the case of CRL, shown in Figure 1, a  $\alpha$ -helix unwinds at one end and extends at the other. Following this rearrangement, the surface characteristics in the proximity of the active site change radically. In the closed state, the side of the loop facing the solvent is hydrophilic. When the lid moves aside, several hydrophobic side chains are exposed to the solvent. A large hydrophobic pocket containing the active site is exposed to the environment. In this conformation, the nucleophilic serine is easily accessible. In this way, lipases are strongly adsorbed to hydrophobic interfaces through several pockets of a large hydrophobic surface, which surrounds the catalytic side. The catalytic triad is now accessible to the substrate and the lipase can exert its lipolytic activity. The lid is held in place by mostly hydrophobic and some hydrogen bonds. The structure of the lid differs for lipases in the number and position of the surface loops. In some cases, the lid is very small and does not completely seclude the active center from the medium, so that the closed form is partially active [21]. In other cases, the loop structure is very complex and the closed form of the lipase is completely inactive [22].

#### 2.4. Enzymatic Biodiesel Production

Lipases are ubiquitously present in plants, animals and microorganisms (bacteria, fungi and yeasts). Microbial lipases are mostly used in industry since they are more stable and available in bulk at lower cost [23].

Lipases can be divided into three groups: 1,3-specific, fatty acid-specific and non-specific lipases. The 1,3-specific lipases hydrolyze ester bonds in the position 1 and 3 of triglycerides. The fatty acid-specific lipases hydrolyze esters of long-chain fatty acids with double bonds in cis-position at C9. The non-specific lipases randomly cleave the acylglycerols. For biodiesel production, lipases should be non-specific to efficiently catalyze the transesterification of triglycerides in fatty acid alkyl-esters.

Enzymes used for commercial applications are frequently immobilized. Among them, *Candida antartica* lipase immobilized on acrylic resin (Novozym<sup>®</sup> 435) [24], *Mucor miehei* lipase immobilized on a macroporous ion-exchange resin (Lipozyme IM) [25], *Thermomyces lanuginosus* lipase (TTL) immobilized on acrylic resin (Lipozyme TL IM) [26] and *Rhizomucor miehei* lipase immobilized on macroporous anion exchange resin (Lipozyme RM IM) [27]. Most studies on bacterial lipases for biodiesel production concern *Burkholderia cepacia* lipase (BCL) [28] and *Pseudomonas fluorescens* lipase [29]. *Candida antarctica* lipase B (CALB) is the most widely applied lipase from yeast for biodiesel production. *Candida rugosa* lipase has also been used [30]. Lipases from fungi used in transesterification include *Thermomyces lanuginosus* lipase (TLL), *Rhizopus oryzae* lipase (ROL) [31], *Penicillium expansum* lipase (PEL) [32] and *Geotrichum sp.* lipase (GSL) [33]. The information regarding the sources of lipase used for the production of biodiesel are summarized in Table 1.

**Table 1.** Sources of lipase used in biodiesel production.

Source	Brand Name	Reference
<i>Candida antartica</i>	Novozym <sup>®</sup> 435	[24]
<i>Mucor miehei</i>	Lipozyme IM	[25]
<i>Thermomyces lanuginosus</i>	Lipozyme TL IM	[26]
<i>Rhizomucor miehei</i>	Lipozyme RM IM	[27]
<i>Burkholderia cepacia</i>	-	[28]
<i>Pseudomonas fluorescens</i>	-	[29]
<i>Candida rugose</i>	-	[30]
<i>Rhizopus oryzae</i>	-	[31]
<i>Penicillium expansum</i>	-	[32]
<i>Geotrichum sp.</i>	-	[33]

- Not commercialized.

The major drawback to the industrial production of enzymatic biodiesel is the high cost of the enzymes. However, the enzymatic process can use cheap and low-quality feedstock (waste frying oil, non-edible oil, waste restaurant oil, yellow grease, lard, animal fats and algae) with high free fatty acid content, which can significantly reduce the total production cost [34]. The cost of the immobilization support is another important issue. Actually, many technologies have been developed for lipase immobilization, but only a few are industrialized due to the high cost of the immobilization process (see Table 1). Progress in the development of innovative, inexpensive immobilization techniques with low reaction time, higher enzyme stability and activity and low-cost supports need to be developed for large-scale enzymatic biodiesel production.

### 3. Mesoporous Silica Supports

Mesoporous silicates are promising candidates for enzyme immobilization with respect to the requirements for enzyme supports, such as large surface area, narrow pore size distribution, well-defined pore geometry, thermal and mechanical stability, sufficient functional groups for enzyme attachment (hydroxyl-groups which can be activated allowing for linking the enzyme [35,36]), water insolubility, regenerability and toxicological safety.

### 3.1. Sol-Gel Silica

The sol-gel process is a main technique for producing mesoporous silica supports, which as highlighted above are suited for enzyme immobilization. The sol-gel process is carried out at low temperature close to room temperature using organometallic compounds, solvent and catalyst. It is based on hydrolysis and polycondensation reactions of organometallic compounds [37]. Through these reactions, the system evolves from a colloidal solution called sol into an integrated, semi-solid three-dimensional structure network called a gel [38], in which the liquid phase (solvents, catalysts) are trapped in the interstices. Then, the gel goes through two more processes: ageing and drying. The latter can be carried out at room temperature, producing a xerogel [39], or using a gas (such as CO<sub>2</sub>) in supercritical conditions, obtaining an aerogel [40]. Aerogels and xerogels have a dendritic microstructure, in which spherical particles of an average size of 2–5 nm are fused to form a cluster. These clusters form a highly porous three-dimensional structure with nearly fractal-shaped chains, with pores smaller than 100 nm. The average size and density of the pores can be controlled during the manufacturing process. They have average pore diameters in the mesopore (2–50 nm) and/or micropore ( $\leq 2$  nm) range, and surface areas ranging from about 100 to 1000 m<sup>2</sup> g<sup>-1</sup>. This means that about half of the atoms in the gel are on the surface. Thanks to mild conditions of sol-gel synthesis, it can be used for one-pot enzyme entrapment, as illustrated in Figure 2. The advantages of this method are related to both the features of the support, such as uniformity, high purity, large surface area and great pore volume, and to the mild processing conditions, which should not cause any injury to the enzyme [41–43]. After entrapment, the enzyme is not attached to the support, but the support acts as a physical barrier to its diffusion.

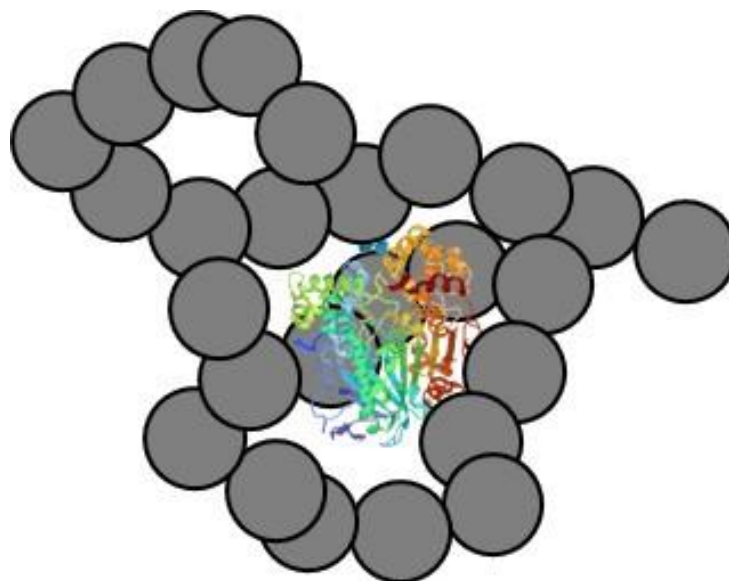


**Figure 2.** Schematic illustration of lipase entrapped in sol-gel silica (xerogel, aerogel).

An alternative method for support enhancement in enzymatic immobilization is the modification of a silica surface support using an ionic liquid as an additive. The application of an additive in the gel structure has the aim to increase surface area and pore size and to enhance the protective hydration layer on the enzyme, which prevents enzyme denaturation in the presence of alcohol [44–46]. Protic ionic liquids (PIL) are the result of the combination of an acid and a Brønsted base, presenting high proton mobility, low cost, easy synthesis and low toxicity. It was found that the surface modification of silica with PIL for lipase immobilization by encapsulation positively influences the catalytic efficiency of the different lipases [45,47].

### 3.2. Ordered Mesoporous Silica (OMS)

Many ordered mesoporous silica materials have been synthesized since the Mobil oil company first discovered them in 1992 [48,49]. These new materials (M41S) showed a pore order organization similar to zeolites, but with larger pore size. These peculiar properties allowed new opportunities to use these materials for applications in many fields, such as biomedical [50], catalysis [51], chemical separation and adsorption [52]. The synthesis of this family of mesoporous materials is based on the combination of sol-gel and surfactant (templating) sciences. The templating agent is an organic species that allows the formation of the structure. It self-organizes, forming a crystalline lattice representing the central structure where a material, often inorganic, nucleates and grows [53]. After the removal of the templating structure, its geometric characteristics are replicated in the structure of the inorganic material. The hexagonal structure MCM-41 represents the most thermally stable member of the M41S family and the easiest to produce. It is characterized by highly regular arrays of uniform-sized channels whose diameters are in the range of 15–100 Å. The peculiarities of MCM-41 structure depend on the kind of templates used, the addition of auxiliary organic compounds and the reaction parameters [54,55].

Another main family of the OMS is named Santa Barbara Amorphous no 15 (SBA-15), discovered in 1998 [56]. The templating agent used is amphiphilic triblock copolymers in strong acidic media. SBA-15 has pore size in the range between 5 to 30 nm, possesses a regular hexagonal array of pores with uniform diameter and has a high thermal, mechanical and chemical stability. Particularly important for lipase immobilization is the tuneable pore size in the 5–10 nm range. This renders SBA-15 an ideal support for successful immobilization of lipase, since the pore size can be adjusted to match the molecular diameter of the lipase under study. For physical adsorption, this is particularly relevant, since too big pore size may lead to the leaching of lipases from the channels, causing a decrease in enzyme loading and instability [57,58]. In addition, the thick silica walls, peculiar to this material, makes the SBA-15 stable and resistant. The presence of abundant surface hydroxyl promotes an easy functionalization with hydrophobic groups for lipase adsorption or with reactive groups for covalent linkage.

### 3.3. Mesocellular Silica Foam

Among all possible forms of mesoporous silica particles (MSPs), mesostructured cellular foams (MCF) are suitable for enzyme immobilization thanks to their structure formed by uniform-sized, large spherical cells interconnected by windows, which create a continuous 3D pore system [59]. This three-dimensional network allows a better substance diffusion than a 2D pore structure of conventional MSPs such as SBA-15 or MCM-41 [60]. MCF silica has pore size in the range of 15–50 nm and windows of 10–15 nm. Pore and window sizes of MCF are readily tuneable by adjusting surfactant (template), swelling agent and silica source ratio. The MCF materials resemble aerogels, with their well-defined pore and wall structure, thick walls and high hydrothermal stability, but are easier to synthesize. MCF with large mesopores was prepared in aqueous hydrochloric acid using dilute solutions of the non-ionic block copolymer surfactant Pluronic P123, with 1,3,5-trimethylbenzene (TMB) as the organic swelling agent and tetraethyl orthosilicate (TEOS) as the silica precursor [59]. A comparative study on mesocellular silica foam with different template removal methods and their effects on enzyme immobilization was carried out [61]. They have prepared MCFs using two different template removal methods: calcination and solvent extraction. The first led to a reorganization of the pores, with a more orderly organized pore structure and increased BET surface area due to porous structure collapse. The solvent extraction method allowed for better preserving the random 3D micropore structure.

MCFs are suitable supports for enzyme immobilization. In particular, they are suited for adsorption and crosslinking of the adsorbed enzyme to form cross-linked enzyme aggregates (CLEAs). In fact, the large pores are able to adsorb a large amount of enzyme molecules inside each cavity. Once cross-linked, the CLEAs can no longer move out of the

cavity due to the smaller size of the interconnecting windows. Thanks to this, the desorption of the enzyme from the support is minimized and at the same time, the interconnected structure allows an easy diffusion of reagents and products. MCFs were used to host the CLEAs of glucose oxidase in the cellular pores, resulting in the improvement of catalytic performance of immobilized enzyme [62]. The hydrophobic modified MCFs can provide a promising platform for lipase CLEAs.

#### 3.4. Biomimetic Silica

Biomimetic silica is the *in vitro* silica formation through reactions similar to those occurring *in vivo*. In nature, biomineralization provides a mechanism by which biological organisms generate hard composite materials (e.g., shells) by using proteins as scaffolds for inorganic materials. Biosilicification is the formation of silica particles that occurs, for example, in diatoms. Biosilica nanoparticles can be synthesized using a silica precursor and a wide range of cationic amine-rich molecules as catalyst, i.e., polyethyleneimine (PEI). The reaction rapidly forms a network of porous silica nanospheres that entraps the catalyst and any other material that is contained within the reaction mixture. Hence, the procedure can be used as a mechanism for enzyme entrapment, thanks to the mild reaction conditions (neutral pH and room temperature in aqueous environment) [63]. These conditions are compatible with the retention of enzyme activity. Multiple enzymes have been entrapped with this method [64].

#### 3.5. Silica Nanoflowers

MSPs with radial-oriented mesochannels and a conical pore shape are ideal scaffolds for catalytic applications, as the pore structures are accessible by large molecules. Increases in the center radial structure and pore size enable molecules to move easily into or out of the pores and promote loading and mass transport [65]. These factors can enhance the catalytic performance of immobilized enzymes [66]. These stellate structures are synthesized using the microemulsion technique. Zhang et al. [67] synthesized monodisperse MSPs smaller than 130 nm. The synthesis was performed with a templating sol-gel technique using cetyltrimethylammonium (CTA+) as the templating surfactant and small organic amines (SOAs) as the mineralizing agent. MSPs with tunable porosity of stellate, raspberry or worm-like morphologies were obtained by varying the nature and the concentration of SOA together with an appropriate choice of the cationic surfactant counter-ion. Fibrous silica nanospheres (KCC-1) were prepared using the microwave-assisted hydrothermal technique [68]. The fabrication involved microemulsion formation using cetylpyridinium bromide (CPB) or cetyltrimethylammonium bromide (CTB) as a template and urea in a mixture of cyclohexane, pentanol and water. Nanoparticles of uniform size (from 250 to 450 nm) were obtained. The KCC-1 nanospheres' internal structure was composed of well-defined and ordered fibers coming out from the center of the particles and distributed uniformly in all directions. Dendrimeric fibers arranged in three dimensions formed the spheres, which can allow easy access to the available high surface area. Wrinkled silica nanoparticles (WSNs) with a radial structure, with silica fibers widening radially outward, have been synthesized using a bi-continuous microemulsion phase [69]. WSNs exhibit a radial open pore structure, in which the pore size is maximum at the extremities, and a hierarchical distribution of pores: each wrinkle-forming nanoparticles is a membrane with a mesoporous structure. WSNs were used to immobilize cellulase [70] and  $\beta$ -glucosidase [71,72]. The results demonstrated that this matrix is a very efficient support for the physical adsorption of enzymes: its peculiar morphology created a favorable microenvironment for catalysis, reducing diffusion limitations. A TEM image of WSNs is shown in Figure 3. The image shows spherical particles with diameters of 200–250 nm, whose internal morphology is composed by silica fibers coming out from the center of the particles. The silica fibers spread uniformly in all directions, forming central-radial pores, which widen radially outward.

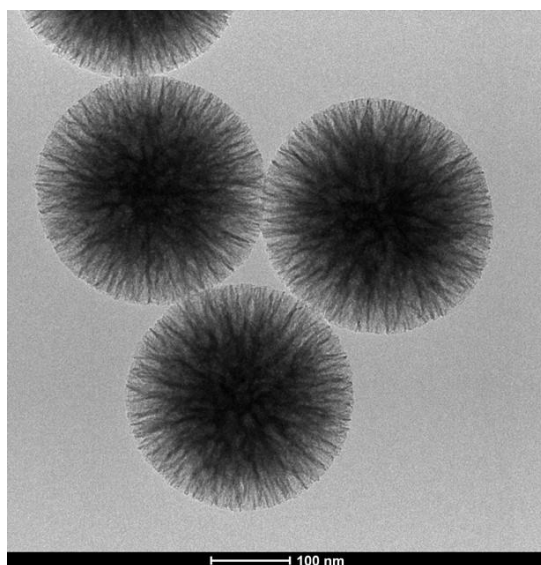


**Figure 3.** TEM image of WSNs.

### 3.6. Non-Surfactant Template Mesoporous Silica

The ordinary surfactants used in the synthesis of mesoporous materials are often expensive and toxic. There have been several attempts to prepare mesoporous silica nanoparticles using non-surfactant templates, such as D-glucose [73], kanemite [74] and boron oxide [75]. However, the pore size of these particles was usually smaller than 4 nm, which is not enough to adsorb bulky enzymes (i.e., lipase or cellulase) in their interior. Recently, Gao et al. [76] synthesized mesoporous silica materials with large interconnected mesopores with tunable pore sizes (6–13 nm) by templating with the green non-surfactant tannic acid (TA). TA is a glycoside polymer of gallic acid present in a large part of plants. TA is cheap and non-toxic, and can be easily removed without calcination, by water or ethanol extraction. Tannic acid templated mesoporous silica nanoparticles (TA-MSNPs) have been used as supports for immobilization of several enzymes, such as lysozyme and bovine serum albumin [76], NHase [77] and  $\beta$ -glucosidase [78]. A TEM image of TA-MSNPs is shown in Figure 4. The image shows quasi-spherical porous particles with a diameter of about 250 nm.

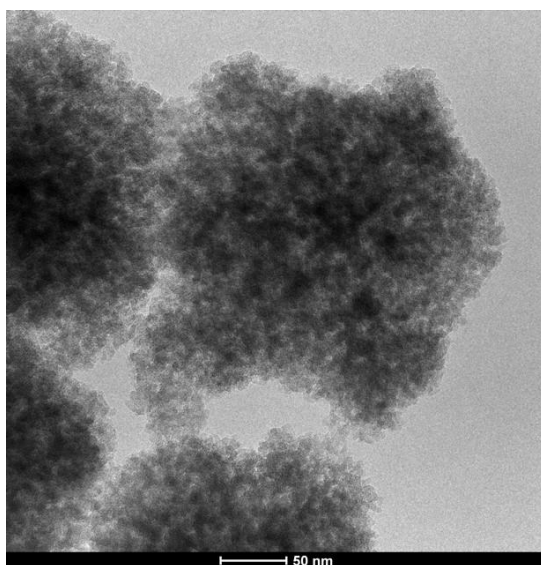


**Figure 4.** TEM image of TA-MSNPs.

### 3.7. Spray-Drying Mesoporous Microparticles

Spray-drying is a versatile methodology for the scalable production of micron-size particles for a broad range of applications. The production of nanostructured particles via spray-drying is of interest because it is simple, economic and can be scaled up to ton quantities [79]. Spray-drying is initiated by atomizing/spraying suspensions into droplets followed by a drying process, resulting in solid particles (see Figure 5). A silica colloidal suspension can be used as a precursor. Colloidal silica is a good precursor for spray-drying because of its stability, its ease of dispersion in water and the possibility to control its size at the nanometer scale. Usually, the precursor is atomized to form spherical droplets, which contains nanometer-sized solid particles. The dispersion water is evaporated inside a reactor, resulting in sub-micrometer-sized nanostructured particles. This technology has also been employed to prepare enzyme catalyst supports for glucose oxidase, horseradish peroxidase and laccase [80].

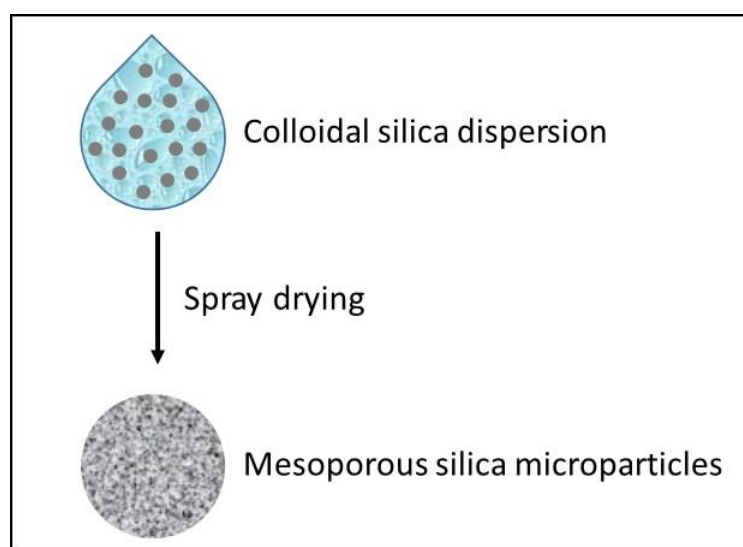


Figure 5. Spray-drying of a colloidal silica dispersion.

### 3.8. Core-Shell Magnetic Silica Particles

In recent decades, magnetic nanoparticles have drawn great attention for practical application as support for enzyme immobilization. Magnetic particles can be easily and quickly separated from the reaction medium by applying an external magnetic field, facilitating the separation of the biocatalyst even in complex and viscous reaction medium, avoiding labor-intensive operations of filtration or centrifugation. However, the bare non-porous magnetic nanoparticles could be damaged due to erosion caused by unwanted interactions with reacting agents [81]. The grafting of a silica layer on magnetic nanocores creates silica composite magnetic nanoparticles, which can prevent the above negative effect [82]. Moreover, the integration of functionalized mesoporous silica materials with magnetically responsive magnetite composites can form porous magnetic nanocomposites, which have the advantages of both mesoporous silica and magnetic nanoparticles. In fact, the mesoporous silica-coated magnetic nanoparticles possess large surface areas, and the mesoporous silica shell can be functionalized easily by organosilanes with different functional groups to generate chemical bonds with enzymes during the immobilization process. There are several reports in the literature reporting fabrication of superparamagnetic ( $\text{Fe}_3\text{O}_4$ ) core and silica shell [83]. Accordingly, the magnetic core-shell structured material seems to be an excellent carrier for the immobilization of lipase [84].

#### 4. Lipase Immobilization

Enzyme immobilization refers to the confinement of the polypeptide molecule onto/within an insoluble support with retention of the enzyme catalytic activity. Techniques for the immobilization are broadly classified into two categories: physical methods (adsorption and entrapment) and chemical methods (covalent binding and cross-linking). Each of these methods has its advantages and problems. Lipases are mainly immobilized by adsorption and covalent coupling [85], although there is no lack of entrapment studies in the literature [86]. Nevertheless, the practical usage of this technique is rather limited. This is because lipases carry out their action mainly at the interface between an aqueous and an oil phase. Entrapment produces restrictions of mass transfer to the lipase active site.

Enzyme immobilization allows the reuse of the biocatalyst. This aspect is very important in the development of industrial processes, given the high cost of enzymes. It is also possible to develop continuous processes, have a greater ease of separation of products (less or not contaminated by proteinaceous material) and an improvement in the characteristics of the enzyme itself, such as thermostability, pH stability and activity [87]. Thermal stability is also an important aspect, as the reaction rate increases with increasing temperature, but enzymes undergo thermal denaturation with loss of their catalytic activity.

##### 4.1. Adsorption

Immobilization by adsorption relies on weak interaction between the enzyme and the support matrix, such as hydrogen bonds, electrostatic forces and hydrophobic interactions. It is the simplest method of enzymatic immobilization, as it only requires the adsorbate and the adsorbent to be put into contact at mild temperatures and without the use of chemical reagents. The activity of the immobilized enzyme is often preserved, and the support can be regenerated. However, due to the weak interactions between the enzyme and the support, leaching of the enzyme into the bulk solution is possible. For lipases, the adsorption technique is advantageous to work in non-aqueous reaction environments, since the solubility of lipase in organic solvent is very low and its desorption from the matrix can be neglected [88]. Lipases are most often immobilized on hydrophobic supports. In aqueous solution, the equilibrium between the open and the closed form of lipase is shifted toward the closed form. Lipases recognize hydrophobic surfaces as if they were at the interface with their own substrate, the oil, and undergo interfacial activation during immobilization, pushing the equilibrium toward the open active form (see Figure 6a). Furthermore, due to the mechanism of interfacial activation, lipases tend to give dimers in aqueous solution, in equilibrium with the monomer, through the interaction of the active centers of two molecules in the open form [89]. The dimeric form is less active than the monomeric one. The immobilization on hydrophobic supports produces a shift of the dimer/monomer equilibrium of the lipase towards the monomer form, which is readily adsorbed in the open form (see Figure 6b). For these reasons, most lipases show a large increase in activity when immobilized on hydrophobic support [90,91].

For biodiesel production, the use of hydrophobic support is desirable. In fact, the accumulation of hydrophilic compounds during the transesterification reaction, i.e., glycerol, can lead to enzyme deactivation. This effect can be reduced using hydrophobic supports [17].

Porous materials are superior sorbents compared to non-porous ones thanks to their larger surface area, provided that the size and morphology of the pores can easily accommodate the enzyme but also allow the easy diffusion of the substrate [92]. In this regard, mesoporous silica is an excellent material for the immobilization of lipase due to the possibility of tailoring the morphology and size of the pores. However, mesoporous silica is quite hydrophilic. Hence, lipase immobilization requires the functionalization of the silica particles with hydrophobic moieties. *Mucor Miehei* (Mm-L) and *Candida rugosa* (CRL) lipase were immobilized on unfunctionalized SBA-15 with similar pore size (8.2 and 8.9 nm, respectively) at pH 6 [93] and 3 [94], respectively. An almost complete conversion of vegetable oil into biodiesel was obtained in 40 and 68 h, respectively. It is possible that

the lipase in acid conditions is already partially deactivated, despite that the adsorption at pH 3 maximizes the immobilization yield due to the establishment of major electrostatic interactions. In fact, it has been shown that when the adsorption is performed at pH 3 and 10, the lipase activity is quenched [95]. In both cases, the second reuse results in a significant loss of activity. For Mm-L, the yield in biodiesel drops to about 50% with the second use and to 15% with the third. For CRL, the biodiesel yield is 42% with the second use. Better results can be obtained by functionalizing mesoporous silica with hydrophobic moieties and finely tuning the pore size to slightly larger than lipase molecular diameter. Octadecyl-modified mesoporous silica nanoparticles (C18-MSNs) with a high C18 content (~19 wt %) and tunable pore sizes (1.6–13 nm) and surface area (219–349 m<sup>2</sup> g<sup>-1</sup>) were synthesized and used for adsorption of CRL [96]. Lipase loading varied from 114 to 1415 mg/g of support. All immobilized CRLs exhibited improved activities compared with the soluble enzyme (see Table 2), suggesting interfacial activation on/in the hydrophobic support and the catalytic activity increased with the pore size. However, the biocatalyst with the pore size slightly larger (4.6 nm) than the molecular size of lipase (3.3 × 4.2 × 5 nm) showed the best stability, retaining 93% of its activity after five reuses. It was demonstrated that hydrophobicity associated with the C18 content is the key for hyperactivation of lipase and pore-size optimization minimized the lipase leaching.

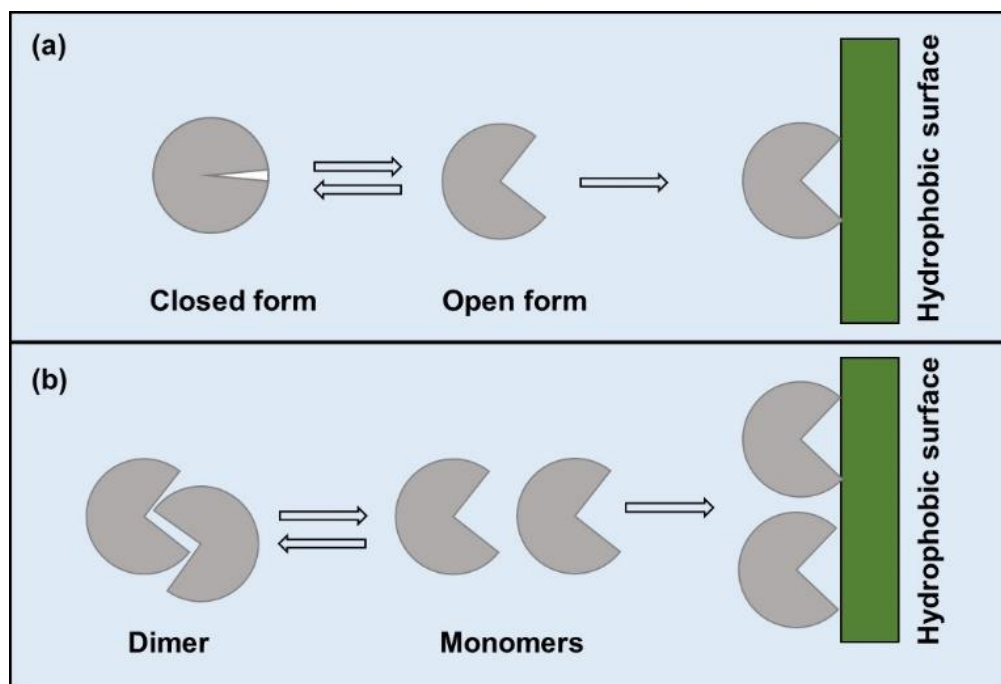


**Figure 6.** Equilibrium closed/open form (a) and dimer/monomer (b) of lipase in the presence of a hydrophobic surface.

**Table 2.** Variation of activity and operational stability of C18-MSNs immobilized lipase with pore size.

Pore Diameter (nm)	Specific Activity with Respect to Soluble Enzyme (times)	Residual Activity after 5 Reuses (%)
1.6	4.51	11
2.0	4.39	12
4.8	5.23	93
6.9	5.70	68
8.0	5.94	54
13	6.12	49

In a following work [97], the same research group states that the small particle size (about 60 nm) and the high preparation cost restrict the application of C18-MSNs in practical catalysis reactors, such as continuous flow devices, despite the high degree of hyperactivation. They developed mesoporous silica microspheres (MSMs) with high hydrophobicity by spray-drying of colloidal silica followed by alkyl chain grafting. The catalysts were optimized in terms of alkyl chain length and enzyme loading. The best catalyst was obtained by functionalizing MSNs with octadecyl trimethoxysilane (pore size 8.6 nm and surface area  $124 \text{ m}^2 \text{ g}^{-1}$ ) and a loading of 100 mg/g of support. Higher lipase loading resulted in a considerable decrease in the relative activity due to pore blocking. The optimized catalyst displayed enzyme hyperactivity of 1.14 times the activity of soluble lipase. When applied to a continuous transesterification reactor for biodiesel production, it demonstrated a high conversion of 99% and a good activity retention of 64% after 24 h.

Lipase from *Thermomyces lanuginosus* (TLL) was immobilized by adsorption on core-shell mesoporous silica functionalized with ionic silsesquioxanes with long-chain counterions (stearate) [98]. The grafting method was employed to incorporate the ionic silsesquioxane containing the positively charged 1,4-diazoniabicyclo[2.2.2]octane group with chloride as a counter-ion. The hydrophobic moiety (stearate anion) was incorporated by ion exchange. The functionalized support is schematized in Figure 7. The modification with the ionic silsesquioxane and stearate led to a shift in pore size from 9.3 to 8.0 nm, still enough to accommodate TLL of about 5 nm molecular diameter. The surface area shifted from 143 to  $61 \text{ m}^2 \text{ g}^{-1}$ . The immobilization yield increased from 36% to 97.4%. Oddly, lipase immobilized on the functionalized support did not show hyperactivation, whereas lipase immobilized on the unfunctionalized hydrophilic support did. The hyperactivation on the hydrophilic support was attributed to the weak interactions between lipase and the silica surface, allowing better preservation of enzyme conformation and easy substrate access to the catalytic site, whereas the hydrophobicity might hamper substrate access to the catalytic site of the enzyme. Nevertheless, the hydrophobic support showed a higher immobilization yield (97% vs. 36%) and better reusability, retaining 76% of lipase initial activity after three reuses vs. 50% after two reuses of lipase on the hydrophilic support.

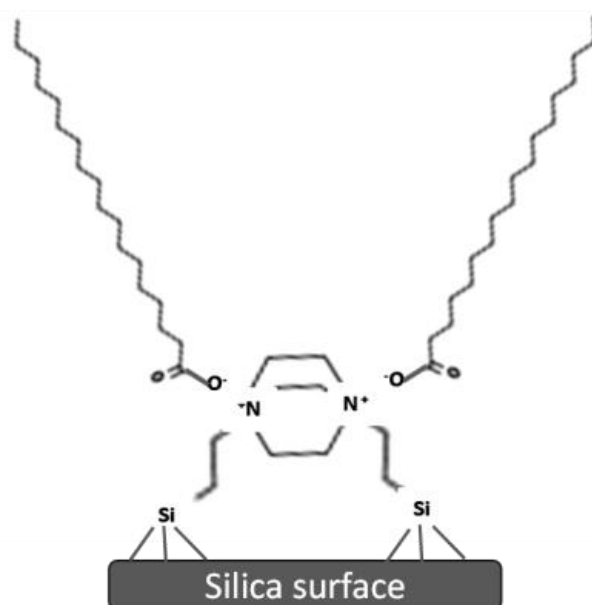
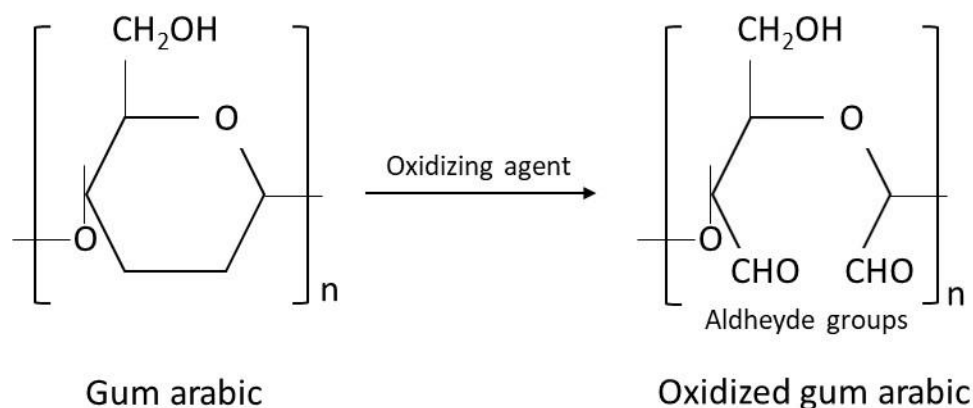


**Figure 7.** Representation of ionic silsesquioxane having stearate as a counter-ion grafted on the silica surface.

Functionalization of silica aerogel with hydrophobic protic ionic liquid (aerogel-IL) was also explored [99]. Lipase from *Burkholderia cepacia* (BCL) was immobilized by adsorption in N-methyl pentanoate monoethanolamine-modified silica aerogel. The incorporation

of the ionic liquid was performed during the sol-gel synthesis process. The performance of the biocatalyst was assayed in the hydrolysis of olive oil emulsion and compared with that of a biocatalyst prepared without the addition of ionic liquid. The aerogel-IL support showed higher yield of immobilization, due to the increase of the surface area from 81 to 322 m<sup>2</sup> g<sup>-1</sup>, pore volume size from 0.04 to 0.8 cm<sup>3</sup> g<sup>-1</sup> and pore diameter from 1.1 to 5.0 nm, and the probable increase in the hydrophobic nature of aerogel due the ionic liquid chemical modification with respect to the unmodified support. BCL immobilized on the aerogel-IL support aerogel increased the reaction rate by about 23.6%. This increase was attributed to the interfacial activation of the lipase retained in the support, maintaining the active site more exposed to the substrate. The optimum temperature of both immobilized biocatalysts shifted from 50 °C of free lipase to 40 °C, resulting in a lower activation energy of the enzyme.

As already mentioned, one of the problems affecting the immobilization by adsorption of the lipase, especially for use in aqueous solvents, is the desorption of the enzyme from the support. This produces a decrease in the activity of the immobilized biocatalyst and the contamination of the reaction environment with proteinaceous material [100]. The situation improves when the lipase is immobilized on hydrophobic materials and the biocatalyst designed to work in an organic environment. However, even in these circumstances, given the weak interactions involved, detachment of the protein from the support cannot be ruled out, especially considering that lipase-catalyzed reactions often lead to products with surfactant properties, able to release the enzyme from the support [101]. A possible strategy to prevent enzyme leaching is the cross-linking of the adsorbed enzyme. This methodology proceeds in two-steps: adsorption and subsequent enzyme cross-linking, which effectively prevents the leaching of cross-linked enzyme aggregates (CLEAs) from the porous support. Obviously, the pores of the support must be large enough to accommodate several enzyme molecules to be cross-linked. Among protein cross-linkers, glutaraldehyde (GA) has been extensively used due to low cost and easy availability [102]. However, GA is toxic and often causes the loss of enzymatic activity. Different macromolecular cross-linkers can be used to replace GA in the preparation of CLEAs. Lipase from *Rhizopus chinensis* was immobilized onto octyl-modified mesocellular foams (MCFs-C8) with pore size of about 32 nm and pore windows of 9.8 nm [103]. Surface area was 1174 m<sup>2</sup> g<sup>-1</sup>. The immobilization was carried out via a two-step process of enzyme adsorption and cross-linking. Oxidized gum Arabic (Scheme 3) was used as a cross-linker to improve the catalytic performance in non-aqueous phase. The catalytic performance of the biocatalyst was compared with those of simply adsorbed lipase and lipase adsorbed and cross-linked with GA. All samples showed hyperactivation with respect to soluble lipase, but the biocatalyst prepared with oxidized gum Arabic showed the highest esterification activity, thermal stability in n-heptane and activity recovery (70% after 5 reuses).



**Scheme 3.** Preparation of oxidized gum Arabic.

The increased activity was attributed to the polyhydroxy structure of the macromolecular polysaccharide, which preserves the hydration layer of lipase, essential for its catalytic activity [104]. In addition, gum Arabic probably affects the interfacial activation of lipase [105]. Improved thermal stability was explained by the confinement effect, i.e., the enhanced enzyme stability in crowded nano-environment: if confined in nanopore that mimics the crowded environment in cells, proteins can give enhanced stability [106]. Similar results were obtained for *Candida antarctica* lipase (CALB) physically adsorbed into MCFs-C8 and cross-linked with oxidized sodium alginate, employed for biodiesel production through the transesterification of soybean oil with methanol [107]. A scheme of lipase adsorption and cross-linking in MCF is shown in Figure 8.

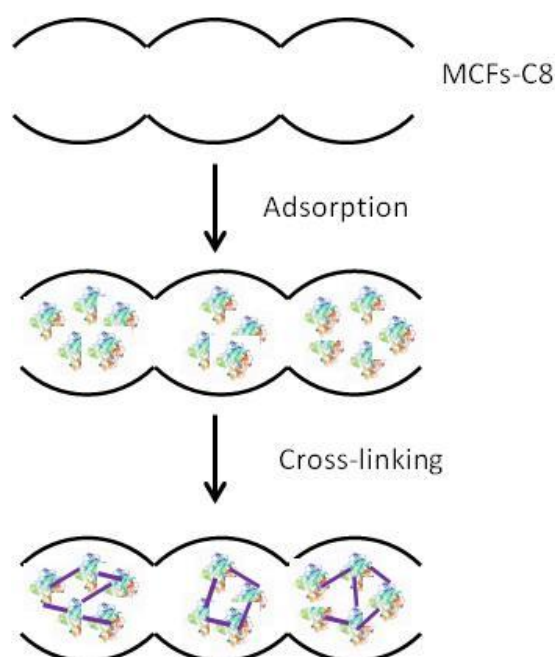


Figure 8. Lipase adsorption and cross-linking in MCF.

Other research groups have dealt with solving diffusion limitations using mesoporous silica supports with particular pore geometries. Actually, catalysis with immobilized enzymes suffers various diffusion limitations imposed by substrates and products. The substrate has to reach the active site of the enzyme by diffusion and at the same time, the products should diffuse away from the active site, assisting further binding of substrate [108]. For porous materials, the situation is more complex since the reactants and products have to diffuse through the pores of the support. Jiang et al. [109] synthesized hierarchically ordered macroporous/mesoporous silica (3DOM/m-S) through the dual-templating method using polystyrene colloidal crystals as the hard template and amphiphilic triblock copolymers P123 as the soft template. The achieved 3DOM/m-S possesses ordered macropores of 400 nm with interconnecting windows of about 100 nm and mesopores of 5.1 nm. Surface area was  $245.5 \text{ m}^2 \text{ g}^{-1}$ . The macropores can provide efficient mass transportation, and the mesopores can create an additional surface area for enzyme loading and enzyme–substrate interactions. Actually, it was found that *Candida antarctica* lipase (CALB,  $3 \times 4 \times 5 \text{ nm}$  molecular size) was mostly immobilized inside the mesopore channels rather than on the external surface (loading  $20 \text{ mg/g}$  of support). The matching between the pore size and the CALB molecular size provided strong thermal stability to the biocatalyst, since the conformational mobility of lipase molecules is restricted by the interactions with the channel walls. The immobilized and soluble CALB were used in the esterification between ethanol and fatty acids with different chain length (C6–C18) in cyclohexane. For soluble CALB, the maximum conversion was approximately 70%, while for the immobilized one, it was about 90%. The higher conversions could be ascribed to

enhanced stability and better dispersibility of immobilized CALB, while the free CALB aggregated in organic solvent, which caused diffusion limitations. Compared with CALB immobilized in ordered macroporous materials, the immobilized biocatalyst showed better reusability, retaining 75% conversion vs. 35% after ten reuses. The decrease of conversion rate in the macroporous support could be attributed to the loss of lipase molecules during centrifugation and washing procedures. These results confirmed that CALB immobilized in 3DOM/m-S, whose pore size matches the molecular size of CALB, could protect the enzyme from mechanical inactivation caused by shearing force and prevent enzyme leaching compared with macropore surface adsorption.

Pang et al. [110] immobilized *Candida rugosa* lipase (CRL) on wrinkled silica nanoparticles having highly ordered, radially oriented mesochannels. The synthesis was performed using TEOS as a source of silica, cetyltrimethylammonium bromide (CTAB) as a surfactant and polyvinylpyrrolidone (PVP) as a stabilizing agent of particle growth. Particle size (240 to 540 nm), specific surface areas (490 to 634 m<sup>2</sup> g<sup>-1</sup>) and pore size (7.95–10.01 nm) were varied using different molar ratios of CTAB to PVP. The activity of the immobilized CRL was higher than the free one in all cases. The better performance was attributed to the radially aligned mesopores of WSNs, allowing dispersing active catalytic sites on large internal surface and pores. On the other hand, it was found that the large pore entrance of wrinkled silica reduces the pore block and alleviates diffusion limitations [71]. *Burkholderia cepacia* lipase (BCL) was immobilized on tannic acid template mesoporous silica (TA-MSN) with mean pore size of 10.1 nm and surface area of 447 m<sup>2</sup> g<sup>-1</sup> [111]. This support, with highly large interconnected mesoporous structure, could be more beneficial for adsorption or heterogeneous catalysis than surfactant-templated MSNs with their non-interconnected cylindrical or dendritic pores, since large interconnected pores would provide more accessible internal volume. The enzyme (loading 34 mg/g of support) showed improved thermal stability. Most of the BCL was immobilized inside the pores of the TA-MSN, which provided a sheltered position that rigidified the external backbone of the enzyme molecules, protecting them from thermal damage. The biocatalyst was reused 15 times with minimal loss of conversion capacity (92.39%).

Xiang et al. [112] have synthesized a new type of inorganic–organic nanocomposite material as efficient support for the immobilization of porcine pancreas lipase (PPL). It was obtained combining chitosan (CS) and mesoporous material SBA-15 via functional ionic liquid as the bridging agent between them (SBA-CIL-CS), as shown in Figure 9. The obtained support had a pore size of 6.19 nm and surface area of 45.38 m<sup>2</sup> g<sup>-1</sup>. PPL was immobilized by adsorption on this support, with a loading of 132 mg/g of support.

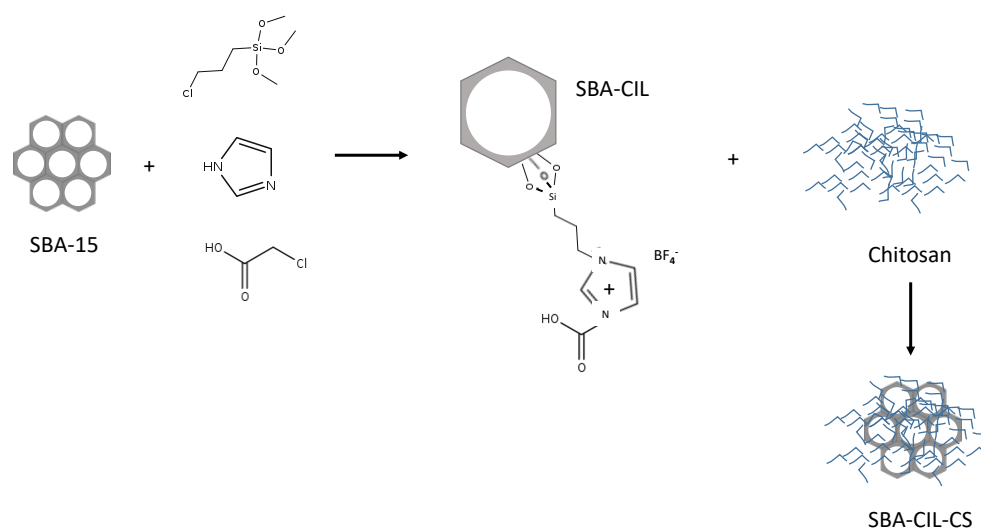


Figure 9. Schematic illustration of the synthesis procedure of SBA-CIL-CS.

The results indicated that SBA-CIL-CS had high immobilization yield and excellent properties, including pH and temperature endurance, activity, stability and reusability (above 82% retention of initial activity after ten cycles). Compared to the soluble enzyme, the relative activity of SBA-CIL-CS-PPL increased to 8.3 times, and 2.3 times more than that of SBA-PPL. This inorganic carrier provided with natural ingredients can protect the secondary structure at the active site of PPL, hindering the conformation change of the enzyme during the immobilization process [101]. With the combination of the advantages of inorganic mesoporous material and natural polymer material, SBA-CIL-CS proved an efficient immobilization support.

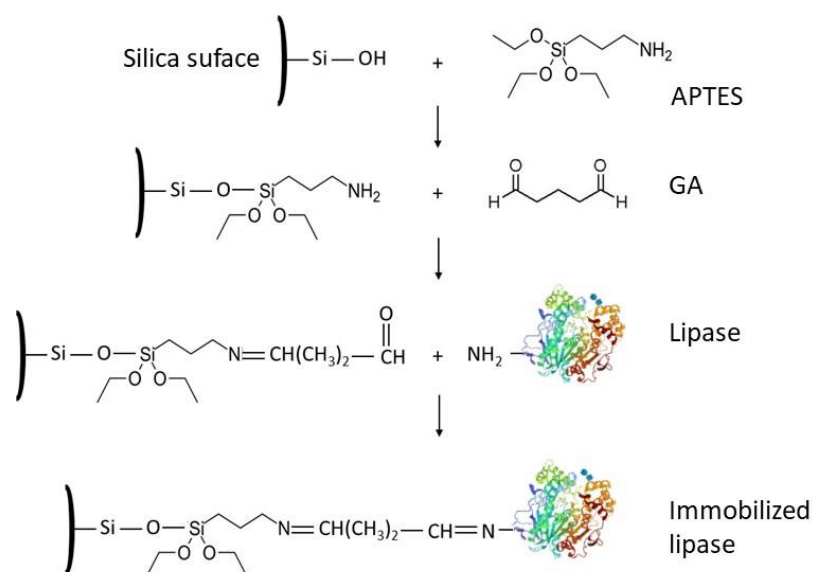
A summary diagram of the commented paper is reported in Table 3.

**Table 3.** Support used and catalyzed reactions for lipase immobilized by adsorption within mesoporous silica particles.

Support	Reaction	Reactants	Solvent	Reference
SBA-15	Transesterification	Rapeseed oil + methanol	-	[93]
SBA-15	Transesterification	Cotton seed oil + methanol	-	[94]
C18-MSN	Hydrolysis	4-nitrophenyl palmitate (pNPP)	Water	[96]
C18-Silica microspheres	Transesterification	Corn oil + methanol	-	[97]
Aerogel-IL	Hydrolysis	Olive oil emulsion	-	[99]
Gum Arabic/MCF	Esterification	Coconut oil + ethanol	-	[103]
Sodium alginate/MCF	Esterification	n-caprylic acid+ethanol	Heptane	[103]
Core shell magnetic silica	Transesterification	Soybean oil + methanol	-	[107]
Hierarchically ordered macro/meso	Hydrolysis	4-nitrophenyl palmitate (pNPP)	Water/isopropanol	[98]
Wrinkled silica	Esterification	Fatty acid + alcohols	Cyclohexane	[109]
TA-MSN	Esterification	Oleic acid + methanol	-	[110]
SBA-15/Chitosan	Esterification	Oleic acid + ethanol	n-hexane	[111]
	Transesterification	Soybean oil + ethanol	n-hexane	[111]
	Hydrolysis	Triacetin	Water	[112]

#### 4.2. Covalent Immobilization

Covalent immobilization is the most common method of lipase immobilization on silica nanoparticles. It involves the formation of a chemical bond between the enzyme and the support. The advantages of this method are the increased lipase stability, increased recyclability and negligible desorption of the enzyme from the support. The enzyme is generally bonded to the surface through one or more sites. However, the activity of lipase is not always retained following covalent immobilization. The ideal immobilization of an enzyme should occur in such a way that it does not destroy the structure of the enzyme nor hinder diffusion of the substrate and product to and from the active site. Silica materials do not possess reactive groups for direct coupling with the enzyme, but rather hydroxyl-groups, which have to be activated. The silica surface can be modified by bifunctional agents or spacer arms (epichlorohydrin, glutaraldehyde, glyoxal, formaldehyde, carbodiimide, ethylenediamine, glycidol, carbonyldiimidazole and others), their function being to promote a strong attachment between the support (silanized or otherwise) and the immobilized enzyme. Bifunctional agents may interact with the groups present on the enzyme, such as hydroxyl, mercapto or amine groups, allowing a larger conformation flexibility for the immobilized system [35,36]. The most common method of activation is the introduction of amino groups on the silica surface, followed by functionalization with reactive groups. A well-established procedure involves the reaction between the surface hydroxyls with (3-Aminopropyl)triethoxysilane (APTES) and the subsequent reaction with glutaraldehyde (GA). GA forms a link with primary amino groups of the functionalized silica nanoparticles and a Schiff base linkage between its aldehyde group and the terminal amino group of lipase, as shown in Scheme 4. Amine groups can be introduced by post-synthesis grafting, or during the synthesis, for example by using a mixture of TEOS and APTS.



**Scheme 4.** Covalent immobilization of lipase on APTES/GA-activated silica surface.

Other functionalization methods consist in the grafting of siloxanes that contain epoxy groups, for example 3-glycidyloxypropyl trimethoxysilane (3-GPTMS). Babaki et al. [113] covalently immobilized lipases from *Candida antarctica* (CALB), *Thermomyces lanuginosus* (TLL) and *Rhizomucor miehei* (RML) onto SBA-15, epoxy-functionalized using 3-GPTMS. The functionalization of SBA-15 and the immobilization of the three lipases were carried out in one step, as reported in Figure 10. The prepared biocatalysts SBA-CALB, SBA-RML and SBA-TLL had enzymatic loading of 36, 36 and 38 mg/g of support, respectively. The enzyme derivatives were used for transesterification of canola oil to fatty acid methyl esters (FAME). All three enzymes were immobilized in high yield onto the modified support. Immobilization onto SBA strongly increased the enzyme thermal stability and methanol tolerance compared to that of the soluble enzymes. Compared to other chemical or physical immobilization methods on the SBA-15 support, epoxy-functionalized silica resulted in higher catalytic activity and reusability. SBA-TLL, SBA-CALB and SBA-RML showed operational stability up to 20, 14 and 7 runs, respectively.

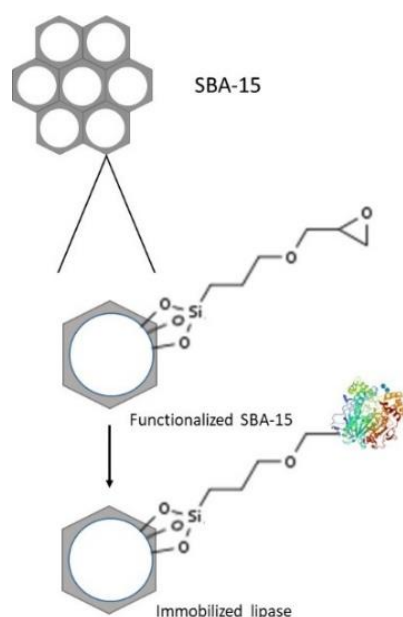


**Figure 10.** Lipase immobilization on epoxy-functionalized SBA-15.

The application of magnetic nanoparticles in enzyme immobilization has received a great deal of attention due to the cheap and easy synthesis and better enzyme performance in recovery and reuse [114]. Core–shell structures of magnetic mesoporous silica that contain a superparamagnetic core and a large surface area provide an improved support system with high capacity and dispersion with external magnetic field [115]. Mehrasbi et al. [116] covalently immobilized lipase from *Candida antarctica* (CALB) on functionalized magnetic nanoparticles to catalyze biodiesel synthesis. Core–shell nanoparticles were synthesized by coating  $\text{Fe}_3\text{O}_4$  nanoparticles, prepared by co-precipitation method, with silica shell ( $\text{Fe}_3\text{O}_4@\text{SiO}_2$ ). Functionalization was obtained using the bifunctional linker 3-GPTMS. The immobilization of CALB was carried out in extremely mild conditions (pH 7.0, 25 °C). The biocatalyst was used for the conversion of waste cooking oil with methanol to FAMES. The protein binding efficiency on functionalized  $\text{Fe}_3\text{O}_4@\text{SiO}_2$  was calculated as 84%, preserving 97% of specific activity of the soluble enzyme, and a significant improvement of its thermal stability and methanol tolerance compared to the soluble enzyme was observed. Moreover, the effect of tert-butanol and water adsorbent addition on the FAMES yield was evaluated and the methyl ester content reached nearly complete conversion. Water adsorbent was added since the esterification of free fatty acids present in the oil produce water in the reaction medium. Excess water in the reaction medium can cause the aggregation of the enzyme, reducing its catalytic activity.

Ali et al. [117] have covalently immobilized *Candida rugosa* lipase (CRL) on two kinds of radially oriented mesochannels: yolk–shell microspheres represented as  $\text{Fe}_3\text{O}_4@\text{SiO}_2@\text{Hollow KCC}$  (Y.S-1) and  $\text{Fe}_3\text{O}_4@\text{SiO}_2@\text{Hollow mSiO}_2$  (Y.S-2). The yolk–shell mesoporous fibrous (Y.S-1) and non-fibrous (Y.S-2) supports were built through a controllable stepwise interface deposition and surfactant-templating co-assembly process, reported in Figure 11. The obtained multifunctional microspheres possess highly accessible mesoporous channels (20–50 nm), high surface area (600–400  $\text{m}^2/\text{g}$ ) and large magnetization (25–29.5  $\text{emu g}^{-1}$ ). The pronounced cavity in the silica shell leaves the surface nanoparticle much more accessible than in typical core–shell structures, and the thin and highly porous silica walls facilitate encapsulation. After amino functionalization, CRL was immobilized using GA as a linker. Through a simple magnetic separation, the CRL on the yolk–shells can be easily recycled and reused without significant loss in activity, even after 15 reuses. The CRL on Y.S-1 and Y.S-2 showed good loading (797–501  $\text{mg/g}$ ), enzyme activity of 1503 and 837  $\text{U/g}$  respectively, high thermal and pH stability and longer storage capability as compared to the soluble lipase. The immobilization of lipase on yolk–shells restricted its freedom to undergo distortion in the stable conformation, stabilizing it against denaturing for a long period of time as compared to the soluble lipase. As can be seen, the CRL on Y.S-1 showed the best loading, activity, thermal, pH and storage stability. This could depend on ordered mesopore channels, radially aligned, in the outer shells of Y.S-1, which allow for hosting a greater amount of CRL, avoiding diffusional limitation.

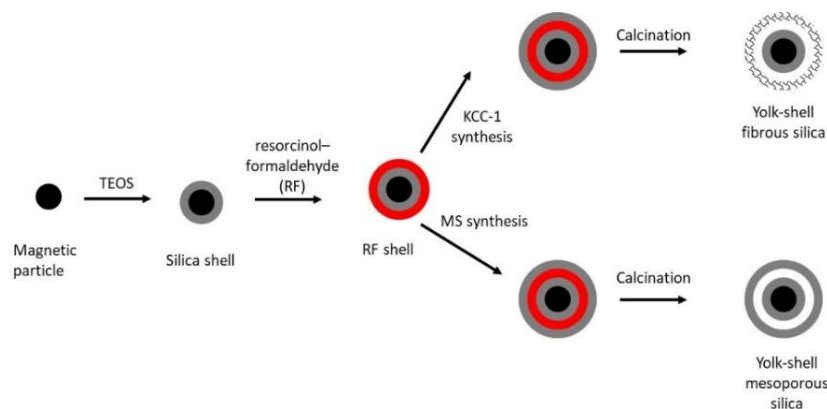


**Figure 11.** Synthesis of yolk–shell hollow fibrous and non-fibrous microspheres.

The same research group [118] covalently immobilized lipase from *Candida rugosa* on paramagnetic amine surface-modified mesoporous fibrous silica ( $\text{Fe}_3\text{O}_4@\text{KCC-1-NH}_2$ ). These nanoparticles had a pore diameter of 10–20 nm and a large surface area of  $370.27 \text{ m}^2 \text{ g}^{-1}$ , providing a large space for lipase loading. Covalent immobilization of CRL was carried out using GA. The obtained biocatalyst had lipase loading of  $283 \text{ mg g}^{-1}$  of carrier. It showed better resistance to temperature and pH inactivation than soluble lipase, expanding the reaction pH and temperature regions. Immobilized CRL showed enzyme activity of  $630 \text{ U g}^{-1}$  and retained 89% of the initial activity after 28 days and 69% after 10 cycles. Esmi et al. [119] immobilized *Rhizopus oryzae* lipase (ROL) on the mesoporous silica magnetic nanoparticles (MNPs@MS) coated with mesoporous silica (MS) functionalized by amine and aldehyde groups. They had a surface area of  $354 \text{ m}^2/\text{g}$ . The nano-biocatalysts were used to produce fatty acid methyl esters in the transesterification reaction of olive oil with methanol. MNPs were synthesized by using the co-precipitation method and coated with MS by sol-gel synthesis using cetyltrimethylammonium bromide (CTAB) as a template for mesoporous formation. ROL was immobilized on these supports via physical adsorption and covalent attachment, as reported in Figure 12. Covalent linkages between MNPs@MS and ROL were created using both APTES and GA. The best biocatalyst is that prepared by covalent linkage (ROL-MNPs@MS-AP-GA). This led to an enzyme loading of 82.4%, the specific activity of  $0.403 \text{ U}/\text{mg}$  and the highest biodiesel yield of 88.4%. This could depend on both limited steric hindrance thanks to Ga functionalization, which provides wider space for immobilization, and improving the mobility of the enzyme during hydrolysis reaction due to the flexible arm of suitable length.

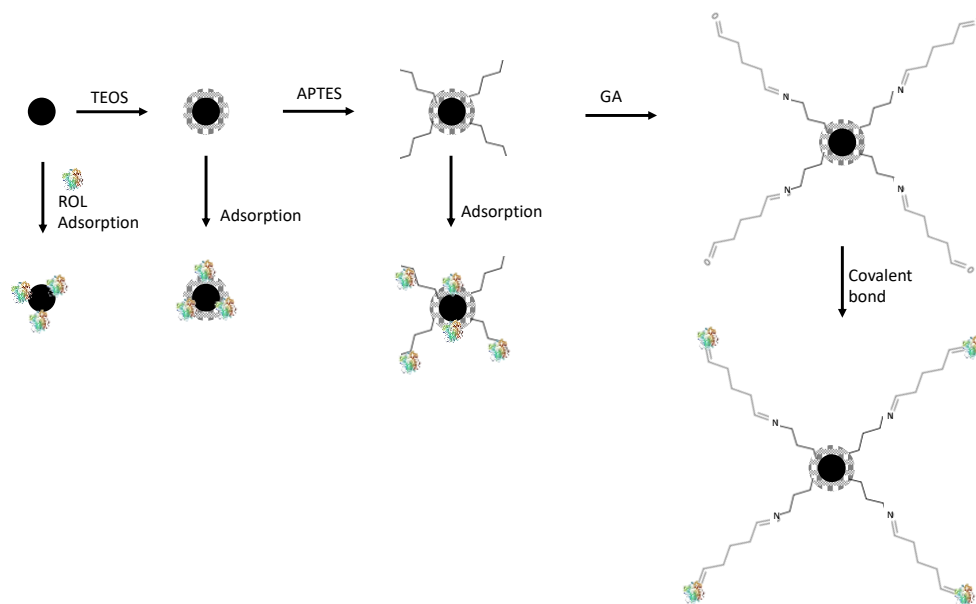


**Figure 12.** Schematic illustration of functionalization of MNPs with APTES and GA and immobilization of ROL.

Khoobbakht et al. [120] immobilized *Burkholderia cepacia* lipase onto mesoporous silica/iron oxide magnetic core–shell nanoparticles for canola waste cooking oil (WCO) conversion to biodiesel. The primary amino groups of microspheres were activated using GA coupling agent for a linkage with the amino acid residue of lipase (see Figure 13). Response surface methodology (RSM) was used to investigate the influence of the experiment variables, consisting of immobilized lipase concentration, reaction time, methanol to WCO molar ratio and reaction temperature, on the biodiesel yield. The obtained results predicted maximum FAMEs content of 92% at immobilized lipase concentration of 36%, reaction time of 25 h, methanol to WCO molar ratio of 6.2 and reaction temperature of  $34 \text{ }^\circ\text{C}$ . The biocatalyst lost only 11% of its initial activity in the third cycle of transesterification.

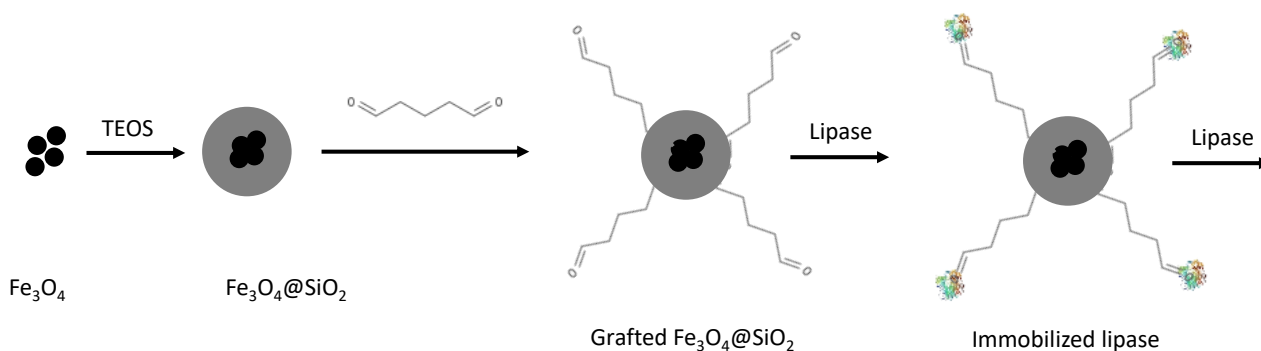


**Figure 13.** Schematic illustration of the synthesis of lipase immobilization on superparamagnetic mesoporous silica-SPION core-shell nanoparticles.

A great interest has evolved in enzyme covalent attachment without a cross-linking agent, complying with the trend of green chemistry. Shao et al. [121] carried out a green and cheap immobilization process of porcine pancreatic lipase (PPL) using three mesoporous magnetic nanoparticles, Fe<sub>3</sub>O<sub>4</sub>@MCM-41, Fe<sub>3</sub>O<sub>4</sub>@MCM-41/CPS (CPS is 3-chloropropyltriethoxysilane) and Fe<sub>3</sub>O<sub>4</sub>@MCM-41/APTS. They had surface areas of 73.85, 12.16 and 12.23 m<sup>2</sup>/g, respectively. PPL was immobilized onto these nanoparticles by covalent attachment, physical adsorption and cross-linking, respectively. In Figure 14, a schematic representation of core-shell Fe<sub>3</sub>O<sub>4</sub>@SiO<sub>2</sub> nanoparticles' formation and the PPL immobilization process is reported. The catalytic studies showed that the best biocatalyst is that obtained by covalent linking without a cross-linking agent. It was obtained by reacting the enzyme with the CPS-functionalized support in phosphate-buffered saline (PBS) solution at pH 7.5 and room temperature. The nitrogen of -NH<sub>2</sub> groups of the enzyme bind covalently to the terminal carbon atom of the propyl, with Cl<sup>-</sup> being the leaving group. It exhibits enhanced immobilization efficiency (maximum 96%), maximum relative activity (up to 96%), high stability and reusability (83% 56 days and 86.7% 10 cycles). This behavior depends on the functional group (chloropropyl) used for the covalent attachment for lipase immobilization, which establishes strong interactions between proteins and carriers [122], which allows for preserving the activity of the enzyme and improving its thermal and operational stability. On the contrary, the cross-linking using GA linker changes the conformation of PPL and results in its deactivation [123]. Moreover, it could also damage some important amino acid residues. Eventually, the physical adsorption preserves the native conformation of the enzyme, but due to weak interaction between the enzyme and support, the biocatalyst is very sensitive to change of the pH and temperature and shows low operational stability.

Efficient immobilization is the result of the perfect matching of several factors depending on the enzyme, the process, the immobilization support and the additives used for modification supports [44,45]. In this frame, Carvalho et al. [124] have focused their attention. They have immobilized lipase from *Burkholderia cepacia* (LBC) onto silica xerogel prepared by a sol-gel technique treated with protic ionic liquid (PIL), N-methylmonoethanolamine pentanoate and bifunctional agents (epichlorohydrin or glutaraldehyde). They had prepared two supports for lipase immobilization, control silica xerogel (SC) and silica xerogel produced with protic ionic liquid (SIL). Lipase immobilized by covalent binding with epichlorohydrin (CBE) on control silica (CBE-SC) and onto silica produced with protic ionic liquid (CBE-SIL). These supports had a surface area of 349.4 and 371 m<sup>2</sup> g<sup>-1</sup>, respectively. The prepared biocatalysts LBC-CBE-SC and LBC-CBE-SIL had enzymatic loading of 349.4 and 371.8 mg/g of support, respectively. Figure 15 shows the possible reaction mechanisms of the silica support with functional activating agents epichlorohydrin and lipase. Evaluations of these potentially useful biocatalysts in hydrolysis and transesterification reactions were performed. The addition of protic ionic liquid (PIL) during the synthesis of the xerogel silica support by a sol-gel method resulted in an improvement in their morphological and

physicochemical characteristics. Bifunctional agents were an important factor in the yield of enzyme immobilization. When epichlorohydrin was used, activity recovery yields of up to 250% were obtained. In addition, biochemical characterization of the immobilized systems under standard reaction conditions was performed (Michaelis–Menten constant, pH and temperature optimum and operational stability in the hydrolysis of olive oil). Further, the potential transesterification activity for three substrates: sunflower, soybean and colza oils, was also determined, achieving a conversion of ethyl esters between 70% and 98%.

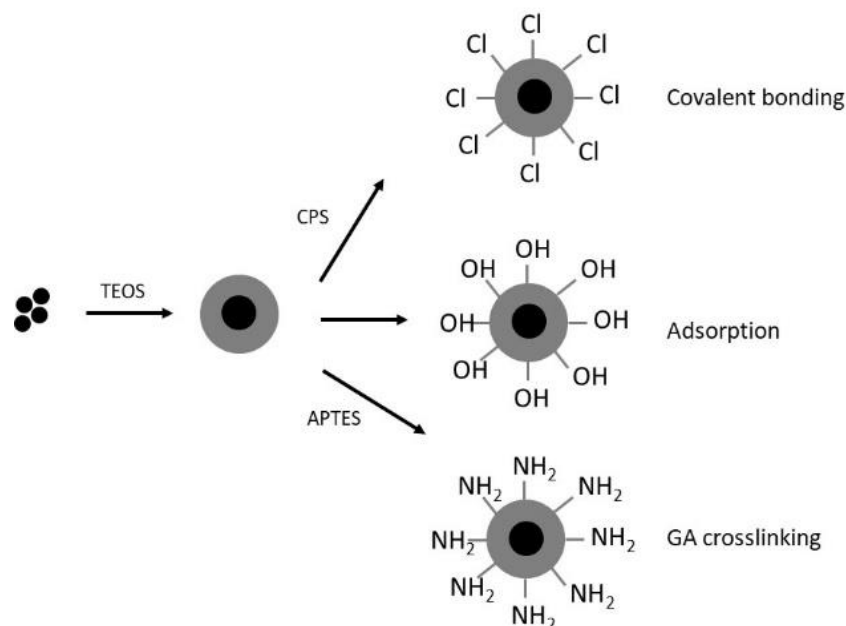


**Figure 14.** Preparation of Fe<sub>3</sub>O<sub>4</sub>@MCM-41/CPS for PPL covalent linking, Fe<sub>3</sub>O<sub>4</sub>@MCM-41 for PPL adsorption and Fe<sub>3</sub>O<sub>4</sub>@MCM-41/APTES for PPL cross-linking with GA.

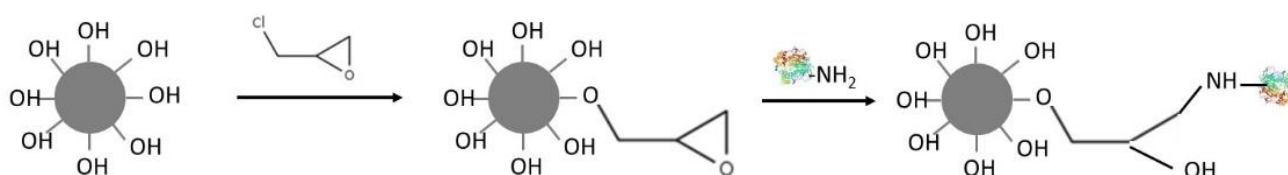


**Figure 15.** Possible mechanism of reaction for silica support with functional activating agents epichlorohydrin and lipase.

#### 4.3. Entrapment

Entrapment is the physical enclosure of enzymes in a confined space, allowing substrates and product diffusion but retaining the enzyme. Immobilization of lipase into silica nanoparticles is usually carried out by the sol-gel method using a silica precursor (i.e., TEOS). However, lipase entrapment poses the problem that the confinement in a small space prevents the contact with the water/oil interface and thus inhibits interfacial activation. Furthermore, the natural substrate of lipase is quite bulky, creating diffusional restrictions. For this reason, there are not many works describing lipase entrapment into silica nanoparticles, and they are mostly focused on the advantages that can be obtained with this type of technique, namely stability and the possibility of reusing the catalyst a good number of times. *Rhizomucor miehei* lipase was entrapped in silica nanoparticles having an oleic acid core (Figure 16) and used as catalysts for transesterification between cottonseed oil and alcohol to obtain biodiesel [125]. The biocatalyst demonstrated good reusability, being employed in 12 consecutive reaction cycles without substantial loss of activity. The immobilized enzyme showed a good storage stability at room temperature,

retaining 100% activity after 6 months, while the native lipase should be stored at 4 °C to maintain its activity. This obviously constitutes a saving in economic terms, as there is no need for low-temperature storage.

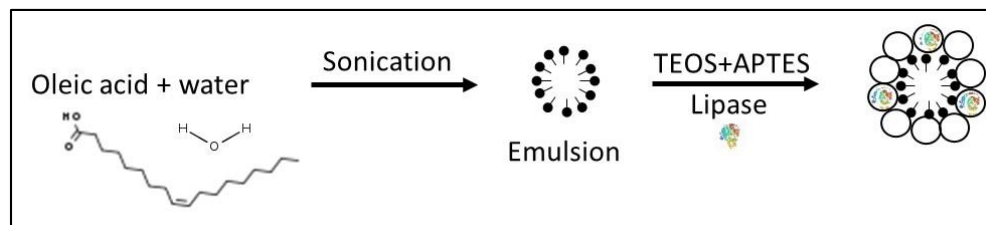


**Figure 16.** Scheme of lipase entrapment within mesoporous silica with an oleic acid core.

*Candida antarctica* B lipase (CALB) was entrapped silica aerogel, showing an increase in thermal, storage and operational stability [126]. However, the stabilization was lower than in the previous case. In fact, the activity dropped to about 50% after 5 months of storage at room temperature. Furthermore, there was a continuous decrease of the activity during reuse of up to 50% after 12 reaction cycles. Cazaban et al. [127] made a comparison between in situ entrapment and adsorption/covalent surface immobilization of *Thermomyces lanuginosus* lipase (TLL) into/on bio-mimetic silica. Entrapment was carried out by mixing tetramethyl orthosilicate (TMOS) polyethyleneimine (PEI) and the enzyme solution at pH 8. Covalent attachment was performed by functionalizing silica particles with octyltrimethoxysilane (OTMS) to provide a hydrophobic environment and (3-Glycidyloxypropyl) methyltriethoxysilane (GMDES) to provide aldehyde groups for covalent linking (see Figure 17). The stability of the biocatalyst obtained by adsorption/covalent linking was similar to the one of the free enzyme, possibly due to the formation of a protein multilayer, where not all the lipase molecules are covalently linked to the support. The biocatalysts obtained by entrapment were much more stable. However, the yield in the synthesis of biodiesel was higher for the lipase immobilized on the silica surface (88% vs. 55%). The biocatalyst obtained by lipase entrapment is probably more affected by diffusional restrictions. Furthermore, a hyperactivation effect of lipase was observed when immobilized on the hetero-functionalized surface of the nanoparticles with a 420% increase in activity, due to the support functionalization with hydrophobic groups.

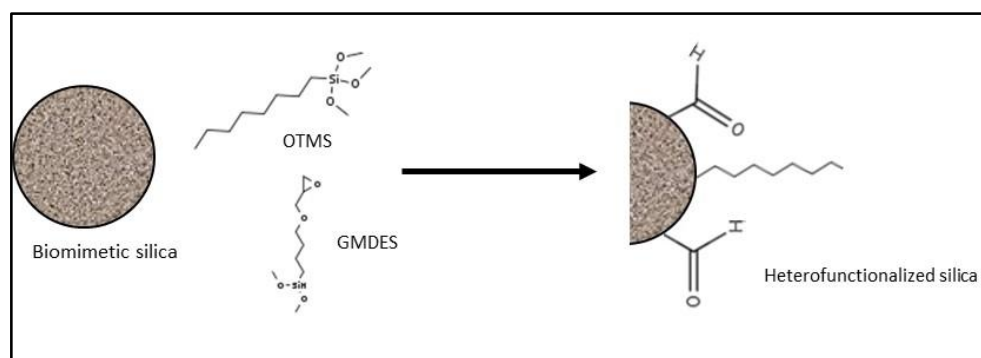


**Figure 17.** Scheme of heterofunctionalization of the biomimetic silica surface.

## 5. Conclusions

In this review, we have focused the attention on the use of lipases for biodiesel production. We have summarized the main results obtained in the production of successful biocatalysts prepared by using several mesoporous supports and by different immobilization procedures. Mesoporous silica materials such as MCF, silica nanoflowers, SBA-15 and core-shell magnetic silica particles have proven to be very suitable for the immobilization of lipase thanks to the great thermal and mechanical stability, controlled textural

characteristics and the presence of abundant surface hydroxyl groups, which allows for easy chemical surface functionalization. Great interest has been addressed to the synthesis of supports formed by functionalized mesoporous silica materials with magnetically responsive magnetite composites, which combine the advantages of both mesoporous silica and magnetic nanoparticles, facilitating the separation of the biocatalyst. Moreover, by combining the properties of natural organic macromolecule materials, i.e., polysaccharide, cellulose, protein, etc., with the properties of inorganic carriers, efficient supports for lipases immobilization can be prepared. We have highlighted the drawbacks connected to the large-scale production of enzymatic biodiesel. In fact, even if the enzymatic process can use cheap and low-quality feedstock with a high free fatty acid content, the cost remains not competitive with the chemical catalysis one, due to the high enzyme costs and those connected to the immobilization procedures. Further studies are needed to overcome the present technological challenges and to lower the enzyme costs, improving the overall process economics towards industrial production of enzymatic biodiesel. Efforts must be addressed in the design and development of innovative, inexpensive immobilization techniques that allow high enzyme stability, preserving its activity.

**Author Contributions:** Writing—original draft preparation, A.C. and V.C.; writing—review and editing, A.C. and V.C. All authors have read and agreed to the published version of the manuscript.

**Funding:** This research received no external funding.

**Data Availability Statement:** No new data were created or analyzed in this study. Data sharing is not applicable to this article.

**Conflicts of Interest:** The authors declare no conflict of interest.

## References

1. Cygler, M.; Schrag, J.D. Structure and conformational flexibility of *Candida rugosa* lipase. *Biochim. Biophys. Acta (BBA) Mol. Cell Biol. Lipids* **1999**, *1441*, 205–214. [[CrossRef](#)]
2. Aguiéiras, E.C.; De Barros, D.S.; Fernandez-Lafuente, R.; Freire, D.M. Production of lipases in cottonseed meal and application of the fermented solid as biocatalyst in esterification and transesterification reactions. *Renew. Energy* **2019**, *130*, 574–581. [[CrossRef](#)]
3. Löfgren, J.; Görbe, T.; Oschmann, M.; Svedendahl Humble, M.; Bäckvall, J.E. Transesterification of a tertiary alcohol by engineered *Candida antarctica* lipase A. *ChemBioChem* **2019**, *20*, 1438–1443. [[CrossRef](#)]
4. Sivakanthan, S.; Jayasooriya, A.P.; Madhujith, T. Optimization of the production of structured lipid by enzymatic interesterification from coconut (*Cocos nucifera*) oil and sesame (*Sesamum indicum*) oil using Response Surface Methodology. *LWT Food Sci. Technol.* **2019**, *101*, 723–730. [[CrossRef](#)]
5. Reis, P.; Holmberg, K.; Watzke, H.; Leser, M.; Miller, R. Lipases at interfaces: A review. *Adv. Colloid Interface Sci.* **2009**, *147–148*, 237–250. [[CrossRef](#)] [[PubMed](#)]
6. Melani, N.B.; Tambourgi, E.B.; Silveira, E. Lipases: From Production to Applications. *Sep. Purif. Rev.* **2020**, *49*, 143–158. [[CrossRef](#)]
7. Sarmah, N.; Revathi, D.; Sheelu, G.; Rani, K.Y.; Sridhar, S.; Mehtab, V.; Sumana, C. Recent advances on sources and industrial applications of lipases. *Biotechnol. Prog.* **2018**, *34*, 5–28. [[CrossRef](#)]
8. Di Iorio, S.; Magno, A.; Mancaruso, E.; Vaglietto, B.; Arnone, L.; Dal Bello, L. *Engine Performance and Emissions of a Small Diesel Engine Fueled with Various Diesel/RME Blends*; SAE Technical Paper; SAE International: Warrendale, PA, USA, 2014. [[CrossRef](#)]
9. Meher, L.; Sagar, D.V.; Naik, S. Technical aspects of biodiesel production by transesterification—A review. *Renew. Sustain. Energy Rev.* **2006**, *10*, 248–268. [[CrossRef](#)]
10. Califano, V.; Bloisi, F.; Perretta, G.; Aronne, A.; Ausanio, G.; Costantini, A.; Vicari, L. Frozen Microemulsions for MAPLE Immobilization of Lipase. *Molecules* **2017**, *22*, 2153. [[CrossRef](#)]
11. Malcata, F.X.; Reyes, H.R.; Garcia, H.S.; Hill, C.G., Jr.; Amundson, C.H. Immobilized lipase reactors for modification of fats and oils—A review. *J. Am. Oil Chem. Soc.* **1990**, *67*, 890–910. [[CrossRef](#)]
12. Knezevic, Z.; Siler-Marinkovic, S.; Mojovic, L. Immobilized lipases as practical catalysts. *Acta Period. Technol.* **2004**, *35*, 151–164. [[CrossRef](#)]
13. Manoel, E.A.; dos Santos, J.C.; Freire, D.M.; Rueda, N.; Fernandez-Lafuente, R. Immobilization of lipases on hydrophobic supports involves the open form of the enzyme. *Enzym. Microb. Technol.* **2015**, *71*, 53–57. [[CrossRef](#)]
14. Tran, N.D.; Balkus, K.J. Perspective of recent progress in immobilization of enzymes. *ACS Catal.* **2011**, *1*, 956–968. [[CrossRef](#)]
15. Zhao, X.; Bao, X.Y.; Guo, W.; Lee, F.Y. Immobilizing catalysts on porous materials. *Mater. Today* **2006**, *9*, 32–39. [[CrossRef](#)]
16. Fernandez-Lafuente, R.; Armisen, P.; Sabuquillo, P.; Fernández-Lorente, G.; Guisán, J.M. Immobilization of lipases by selective adsorption on hydrophobic supports. *Chem. Phys. Lipids* **1998**, *93*, 185–197. [[CrossRef](#)]

17. Rodrigues, R.C.; Virgen-Ortíz, J.J.; Dos Santos, J.C.; Berenguer-Murcia, Á.; Alcantara, A.R.; Barbosa, O.; Ortiz, C.; Fernandez-Lafuente, R. Immobilization of lipases on hydrophobic supports: Immobilization mechanism, advantages, problems, and solutions. *Biotechnol. Adv.* **2019**, *37*, 746–770. [[CrossRef](#)]
18. De María, P.D.; Sánchez-Montero, J.M.; Sinisterra, J.V.; Alcántara, A.R. Understanding *Candida rugosa* lipases: An overview. *Biotechnol. Adv.* **2006**, *24*, 180–196. [[CrossRef](#)]
19. Ollis, D.L.; Cheah, E.; Cygler, M.; Dijkstra, B.W.; Frolow, F.; Franken, S.M.; Harel, M.; Remington, S.J.; Silman, I.; Schrag, J.D.; et al. The alpha/beta hydrolase fold. *Protein Eng.* **1992**, *5*, 197–211. [[CrossRef](#)]
20. Mendes, A.A.; Oliveira, P.C.; de Castro, H.F. Properties and biotechnological applications of porcine pancreatic lipase. *J. Mol. Catal. B Enzym.* **2012**, *78*, 119–134. [[CrossRef](#)]
21. Uppenberg, J.; Hansen, M.T.; Patkar, S.; Jones, T. The sequence, crystal structure determination and refinement of two crystal forms of lipase B from *Candida antarctica*. *Structure* **1994**, *2*, 293–308. [[CrossRef](#)]
22. Carrasco-López, C.; Godoy, C.; Rivas, B.D.L.; Fernández-Lorente, G.; Palomo, J.M.; Guisán, J.M.; Fernández-Lafuente, R.; Martínez-Ripoll, M.; Hermoso, J.A. Activation of Bacterial Thermoalkalophilic Lipases Is Spurred by Dramatic Structural Rearrangements. *J. Biol. Chem.* **2009**, *284*, 4365–4372. [[CrossRef](#)] [[PubMed](#)]
23. Christopher, L.P.; Kumar, H.; Zambare, V.P. Enzymatic biodiesel: Challenges and opportunities. *Appl. Energy* **2014**, *119*, 497–520. [[CrossRef](#)]
24. Lee, K.W.; Min, K.; Park, K.; Yoo, Y.J. Development of an amphiphilic matrix for immobilization of *Candida antarctica* lipase B for biodiesel production. *Biotechnol. Bioprocess Eng.* **2010**, *15*, 603–607. [[CrossRef](#)]
25. Shieh, C.-J.; Liao, H.-F.; Lee, C.-C. Optimization of lipase-catalyzed biodiesel by response surface methodology. *Bioresour. Technol.* **2003**, *88*, 103–106. [[CrossRef](#)]
26. Sim, J.H.; Kamaruddin, A.H.; Bhatia, S. Biodiesel (FAME) Productivity, Catalytic Efficiency and Thermal Stability of Lipozyme TL IM for Crude Palm Oil Transesterification with Methanol. *J. Am. Oil Chem. Soc.* **2010**, *87*, 1027–1034. [[CrossRef](#)]
27. Salis, A.; Pinna, M.; Monduzzi, M.; Solinas, V. Biodiesel production from triolein and short chain alcohols through biocatalysis. *J. Biotechnol.* **2005**, *119*, 291–299. [[CrossRef](#)]
28. Liu, T.; Liu, Y.; Wang, X.; Li, Q.; Wang, J.; Yan, Y. Improving catalytic performance of *Burkholderia cepacia* lipase immobilized on macroporous resin NKA. *J. Mol. Catal. B Enzym.* **2011**, *71*, 45–50. [[CrossRef](#)]
29. Yang, J.; Zhang, B.; Yan, Y. Cloning and Expression of *Pseudomonas fluorescens* 26-2 Lipase Gene in *Pichia pastoris* and Characterizing for Transesterification. *Appl. Biochem. Biotechnol.* **2008**, *159*, 355–365. [[CrossRef](#)] [[PubMed](#)]
30. Shao, P.; Meng, X.; He, J.; Sun, P. Analysis of immobilized *Candida rugosa* lipase catalyzed preparation of biodiesel from rapeseed soapstock. *Food Bioprod. Process.* **2008**, *86*, 283–289. [[CrossRef](#)]
31. Li, Z.; Li, X.; Wang, Y.; Wang, Y.; Wang, F.; Jiang, J. Expression and characterization of recombinant *Rhizopus oryzae* lipase for enzymatic biodiesel production. *Bioresour. Technol.* **2011**, *102*, 9810–9813. [[CrossRef](#)]
32. Zhang, K.-P.; Lai, J.-Q.; Huang, Z.-L.; Yang, Z. *Penicillium expansum* lipase-catalyzed production of biodiesel in ionic liquids. *Bioresour. Technol.* **2011**, *102*, 2767–2772. [[CrossRef](#)] [[PubMed](#)]
33. Yan, J.; Yan, Y.; Liu, S.; Hu, J.; Wang, G. Preparation of cross-linked lipase-coated micro-crystals for biodiesel production from waste cooking oil. *Bioresour. Technol.* **2011**, *102*, 4755–4758. [[CrossRef](#)]
34. Lv, L.; Dai, L.; Du, W.; Liu, D. Progress in Enzymatic Biodiesel Production and Commercialization. *Processes* **2021**, *9*, 355. [[CrossRef](#)]
35. Zhou, Z.; Hartmann, M. Progress in enzyme immobilization in ordered mesoporous materials and related applications. *Chem. Soc. Rev.* **2013**, *42*, 3894–3912. [[CrossRef](#)]
36. Talbert, J.N.; Goddard, J.M. Enzymes on material surfaces. *Colloids Surf. B Biointerfaces* **2012**, *93*, 8–19. [[CrossRef](#)]
37. Silvestri, B.; Guarnieri, D.; Luciani, G.; Costantini, A.; Netti, P.A.; Branda, F. Fluorescent (rhodamine), folate decorated and doxorubicin charged, PEGylated nanoparticles synthesis. *J. Mater. Sci. Mater. Electron.* **2012**, *23*, 1697–1704. [[CrossRef](#)] [[PubMed](#)]
38. Milea, C.A.; Bogatu, C.; Duta, A. The Influence of Parameters in Silica Sol-Gel Process. *Eng. Sci.* **2011**, *4*, 59–66.
39. Soares, C.M.F.; Dos Santos, O.A.; De Castro, H.F.; De Moraes, F.F.; Zanin, G.M. Studies on Immobilized Lipase in Hydrophobic Sol-Gel. *Appl. Biochem. Biotechnol.* **2004**, *113–116*, 307–319. [[CrossRef](#)]
40. Ficanha, A.M.M.; Antunes, A.; Oro, C.E.D.; Valduga, A.T.; Moreira, C.M.; Dallago, R.M.; Mignoni, M. Study of Drying Conditions of the Aerogel Obtained by the Sol-Gel Technique for Immobilization In Situ of Lipase *Candida antarctica* B. *Ind. Biotechnol.* **2019**, *15*, 350–356. [[CrossRef](#)]
41. Vidinha, P.; Augusto, V.; Almeida, M.; Fonseca, I.; Fidalgo, A.; Ilharco, L.; Cabral, J.M.S.; Barreiros, S. Sol-gel encapsulation: An efficient and versatile immobilization technique for cutinase in non-aqueous media. *J. Biotechnol.* **2006**, *121*, 23–33. [[CrossRef](#)] [[PubMed](#)]
42. Zarcuła, C.; Kiss, C.; Corici, L.; Croitoru, R.; Csunderlik, C.; Peter, F. Combined sol-gel entrapment and adsorption method to obtain solid-phase lipase biocatalyst. *Rev. Chim.* **2009**, *60*, 922–927.
43. Tomin, A.; Weiser, D.; Hellner, G.; Bata, Z.; Corici, L.; Péter, F.; Koczka, B.; Poppe, L. Fine-tuning the second generation sol-gel lipase immobilization with ternary alkoxysilane precursor systems. *Process. Biochem.* **2011**, *46*, 52–58. [[CrossRef](#)]
44. Barbosa, A.S.; Lisboa, J.A.; Silva, M.A.O.; Carvalho, N.B.; Pereira, M.M.; Fricks, A.T.; Mattedi, S.; Lima, Á.S.; Franceschi, E.; Soares, C.M.F. The novel mesoporous silica aerogel modified with protic ionic liquid for lipase immobilization. *Quím. Nova* **2016**, *39*, 415–422. [[CrossRef](#)]

45. De Souza, R.L.; de Faria, E.L.P.; Figueiredo, R.T.; Freitas, L.D.S.; Iglesias, M.; Mattedi, S.; Zanin, G.M.; dos Santos, O.A.A.; Coutinho, J.A.; Lima, Á.S.; et al. Protic ionic liquid as additive on lipase immobilization using silica sol–gel. *Enzym. Microb. Technol.* **2013**, *52*, 141–150. [[CrossRef](#)]
46. Zou, B.; Song, C.; Xu, X.; Xia, J.; Huo, S.; Cui, F. Enhancing stabilities of lipase by enzyme aggregate coating immobilized onto ionic liquid modified mesoporous materials. *Appl. Surf. Sci.* **2014**, *311*, 62–67. [[CrossRef](#)]
47. Barbosa, A.D.S.; Silva, M.A.D.O.; Carvalho, N.B.; Mattedi, S.; Iglesias, M.A.; Fricks, A.T.; Lima, Á.S.; Franceschi, E.; Soares, C.M.F. Immobilization of lipase by encapsulation in silica aerogel. *Quím. Nova* **2014**, *37*, 969–976. [[CrossRef](#)]
48. Beck, J.S.; Calabro, D.C.; McCullen, S.B.; Pelrine, B.P.; Schmitt, K.D.; Vartuli, J.C. Catalytic Conversion over Modified Synthetic Mesoporous Crystalline Material. U.S. Patent 5,200,058, 6 April 1993.
49. Beck, J.S.; Calabro, D.C.; McCullen, S.B.; Pelrine, B.P.; Schmitt, K.D.; Vartuli, J.C. Method for Functionalizing Synthetic Mesoporous Crystalline Material. U.S. Patent 2,069,722, 27 May 1992.
50. Silvestri, B.; Pezzella, A.; Luciani, G.; Costantini, A.; Tescione, F.; Branda, F. Heparin conjugated silica nanoparticle synthesis. *Mater. Sci. Eng. C* **2012**, *32*, 2037–2041. [[CrossRef](#)]
51. Parida, K.; Dash, S.S. Manganese containing MCM-41: Synthesis, characterization and catalytic activity in the oxidation of ethylbenzene. *J. Mol. Catal. A Chem.* **2009**, *306*, 54–61. [[CrossRef](#)]
52. Allothman, Z.A.; Apblett, A.W. Metal ion adsorption using polyamine-functionalized mesoporous materials prepared from bromopropyl-functionalized mesoporous silica. *J. Hazard. Mater.* **2010**, *182*, 581–590. [[CrossRef](#)]
53. Di Renzo, F.; Cambon, H.; Dutarte, R. A 28-year-old synthesis of micelle-templated mesoporous silica. *Microporous Mater.* **1997**, *10*, 283–286. [[CrossRef](#)]
54. Beck, J.S.; Vartuli, J.C.; Roth, W.J.; Leonowicz, M.E.; Kresge, C.T.; Schmitt, K.D.; Chu, C.T.W.; Olson, D.H.; Sheppard, E.W.; McCullen, S.B.; et al. A new family of mesoporous molecular sieves prepared with liquid crystal templates. *J. Am. Chem. Soc.* **1992**, *114*, 10834–10843. [[CrossRef](#)]
55. Yang, X.; Zhang, S.; Qiu, Z.; Tian, G.; Feng, Y.; Xiao, F.-S. Stable Ordered Mesoporous Silica Materials Templated by High-Temperature Stable Surfactant Micelle in Alkaline Media. *J. Phys. Chem. B* **2004**, *108*, 4696–4700. [[CrossRef](#)]
56. Zhao, D.Y.; Feng, J.L.; Huo, Q.S.; Melosh, N.; Fredrickson, G.H.; Chmelka, B.F.; Stucky, G.D. Triblock copolymer syntheses of mesoporous silica with periodic 50–300 angstrom pores. *Science* **1998**, *279*, 548–552. [[CrossRef](#)] [[PubMed](#)]
57. Verma, M.L.; Barrow, C.J.; Puri, M. Nanobiotechnology as a novel paradigm for enzyme immobilisation and stabilisation with potential applications in biodiesel production. *Appl. Microbiol. Biotechnol.* **2013**, *97*, 23–39. [[CrossRef](#)]
58. Takahashi, H.; Li, B.; Sasaki, T.; Miyazaki, C.; Kajino, T.; Inagaki, S. Immobilized enzymes in ordered mesoporous silica materials and improvement of their stability and catalytic activity in an organic solvent. *Microporous Mesoporous Mater.* **2001**, *44*, 755–762. [[CrossRef](#)]
59. Schmidt-Winkel, P.; Lukens, W.W.; Yang, P.; Margolese, D.I.; Lettow, J.S.; Ying, J.Y.; Stucky, G.D. Microemulsion Templating of Siliceous Mesostructured Cellular Foams with Well-Defined Ultralarge Mesopores. *Chem. Mater.* **2000**, *12*, 686–696. [[CrossRef](#)]
60. Han, Y.-J.; Watson, J.T.; Stucky, G.D.; Butler, A. Catalytic activity of mesoporous silicate-immobilized chloroperoxidase. *J. Mol. Catal. B Enzym.* **2002**, *17*, 1–8. [[CrossRef](#)]
61. Thananukul, N.; Phongphut, A.; Prichanont, S.; Thanachayanont, C.; Fearn, S.; Chayasombat, B. A comparative study on mesocellular foam silica with different template removal methods and their effects on enzyme immobilization. *J. Porous Mater.* **2018**, *26*, 1059–1068. [[CrossRef](#)]
62. Jung, D.; Paradiso, M.; Hartmann, M. Formation of cross-linked glucose oxidase aggregates in mesocellular foams. *J. Mater. Sci.* **2009**, *44*, 6747–6753. [[CrossRef](#)]
63. Betancor, L.; Luckarift, H.R. Bioinspired enzyme encapsulation for biocatalysis. *Trends Biotechnol.* **2008**, *26*, 566–572. [[CrossRef](#)] [[PubMed](#)]
64. Begum, G.; Goodwin, W.B.; Deglee, B.M.; Sandhage, K.H.; Kröger, N. Compartmentalisation of enzymes for cascade reactions through biomimetic layer-by-layer mineralization. *J. Mater. Chem. B* **2015**, *3*, 5232–5240. [[CrossRef](#)]
65. Wang, Y.; Du, X.; Liu, Z.; Shi, S.; Lv, H. Dendritic fibrous nano-particles (DFNPs): Rising stars of mesoporous materials. *J. Mater. Chem. A* **2019**, *7*, 5111–5152. [[CrossRef](#)]
66. Califano, V.; Costantini, A.; Silvestri, B.; Venezia, V.; Cimino, S.; Sannino, F. The effect of pore morphology on the catalytic performance of  $\beta$ -glucosidase immobilized into mesoporous silica. *Pure Appl. Chem.* **2019**, *91*, 1583–1592. [[CrossRef](#)]
67. Zhang, K.; Xu, L.-L.; Jiang, J.-G.; Calin, N.; Lam, K.-F.; Zhang, S.-J.; Wu, H.-H.; Wu, G.-D.; Albela, B.; Bonneviot, L.; et al. Facile Large-Scale Synthesis of Monodisperse Mesoporous Silica Nanospheres with Tunable Pore Structure. *J. Am. Chem. Soc.* **2013**, *135*, 2427–2430. [[CrossRef](#)]
68. Polshettiwar, V.; Cha, D.K.; Zhang, X.; Basset, J.M. High-Surface-Area Silica Nanospheres (KCC-1) with a Fibrous Morphology. *Angew. Chem. Int. Ed.* **2010**, *49*, 9652–9656. [[CrossRef](#)] [[PubMed](#)]
69. Moon, D.-S.; Lee, J.-K. Tunable Synthesis of Hierarchical Mesoporous Silica Nanoparticles with Radial Wrinkle Structure. *Langmuir* **2012**, *28*, 12341–12347. [[CrossRef](#)]
70. Costantini, A.; Venezia, V.; Pota, G.; Bifulco, A.; Califano, V.; Sannino, F. Adsorption of cellulase on wrinkled silica nanoparticles with enhanced inter-wrinkle distance. *Nanomaterials* **2020**, *10*, 1799. [[CrossRef](#)]
71. Califano, V.; Sannino, F.; Costantini, A.; Avossa, J.; Cimino, S.; Aronne, A. Wrinkled Silica Nanoparticles: Efficient Matrix for  $\beta$ -Glucosidase Immobilization. *J. Phys. Chem. C* **2018**, *122*, 8373–8379. [[CrossRef](#)]

72. Sannino, F.; Costantini, A.; Ruffo, F.; Aronne, A.; Venezia, V.; Califano, V. Covalent Immobilization of  $\beta$ -Glucosidase into Mesoporous Silica Nanoparticles from Anhydrous Acetone Enhances Its Catalytic Performance. *Nanomaterials* **2020**, *10*, 108. [CrossRef]
73. Wei, Y.; Xu, J.; Dong, H.; Dong, J.H.; Qiu, K.; Jansen-Varnum, S.A. Preparation and Physisorption Characterization of d-Glucose-Templated Mesoporous Silica Sol–Gel Materials. *Chem. Mater.* **1999**, *11*, 2023–2029. [CrossRef]
74. Yanagisawa, T.; Shimizu, T.; Kuroda, K.; Kato, C. The Preparation of Alkyltrimethylammonium–Kanemite Complexes and Their Conversion to Microporous Materials. *Bull. Chem. Soc. Jpn.* **1990**, *63*, 988–992. [CrossRef]
75. Baú, L.; Bártová, B.; Arduini, M.; Mancin, F. Surfactant-free synthesis of mesoporous and hollow silicananoparticles with an inorganic template. *Chem. Commun.* **2009**, 7584–7586. [CrossRef] [PubMed]
76. Gao, Z.; Zharov, I. Large Pore Mesoporous Silica Nanoparticles by Templating with a Nonsurfactant Molecule, Tannic Acid. *Chem. Mater.* **2014**, *26*, 2030–2037. [CrossRef]
77. Gao, J.-K.; Zhang, Z.-J.; Jiang, Y.-J.; Chen, Y.; Gao, S.-F. Biomimetic-Functionalized, Tannic Acid-Templated Mesoporous Silica as a New Support for Immobilization of NHase. *Molecules* **2017**, *22*, 1597. [CrossRef]
78. Venezia, V.; Sannino, F.; Costantini, A.; Silvestri, B.; Cimino, S.; Califano, V. Mesoporous silica nanoparticles for  $\beta$ -glucosidase immobilization by templating with a green material: Tannic acid. *Microporous Mesoporous Mater.* **2020**, *302*, 110203. [CrossRef]
79. Iskandar, F.; Gradon, L.; Okuyama, K. Control of the morphology of nanostructured particles prepared by the spray drying of a nanoparticle sol. *J. Colloid Interface Sci.* **2003**, *265*, 296–303. [CrossRef]
80. Patel, S.K.S.; Choi, S.H.; Kang, Y.C.; Lee, J.-K. Large-scale aerosol-assisted synthesis of biofriendly Fe<sub>2</sub>O<sub>3</sub> yolk–shell particles: A promising support for enzyme immobilization. *Nanoscale* **2016**, *8*, 6728–6738. [CrossRef] [PubMed]
81. Wu, P.; Zhu, J.; Xu, Z. Template-Assisted Synthesis of Mesoporous Magnetic Nanocomposite Particles. *Adv. Funct. Mater.* **2004**, *14*, 345–351. [CrossRef]
82. Deng, Y.; Qi, D.; Deng, C.; Zhang, A.X.; Zhao, D. Superparamagnetic High-Magnetization Microspheres with an Fe<sub>3</sub>O<sub>4</sub>@SiO<sub>2</sub> Core and Perpendicularly Aligned Mesoporous SiO<sub>2</sub> Shell for Removal of Microcystins. *J. Am. Chem. Soc.* **2008**, *130*, 28–29. [CrossRef]
83. Sen, T.; Bruce, I.J. Mesoporous silica–magnetite nanocomposites: Fabrication, characterisation and applications in biosciences. *Microporous Mesoporous Mater.* **2009**, *120*, 246–251. [CrossRef]
84. Tran, D.-T.; Chen, C.-L.; Chang, J.-S. Immobilization of Burkholderia sp. lipase on a ferric silica nanocomposite for biodiesel production. *J. Biotechnol.* **2012**, *158*, 112–119. [CrossRef]
85. Shuai, W.; Das, R.K.; Naghdi, M.; Brar, S.K.; Verma, M. A review on the important aspects of lipase immobilization on nanomaterials. *Biotechnol. Appl. Biochem.* **2017**, *64*, 496–508. [CrossRef]
86. Ismail, A.R.; Baek, K.-H. Lipase immobilization with support materials, preparation techniques, and applications: Present and future aspects. *Int. J. Biol. Macromol.* **2020**, *163*, 1624–1639. [CrossRef]
87. Mateo, C.; Palomo, J.M.; Fernandez-Lorente, G.; Guisan, J.M.; Fernandez-Lafuente, R. Improvement of enzyme activity, stability and selectivity via immobilization techniques. *Enzyme Microb. Technol.* **2007**, *40*, 1451–1463. [CrossRef]
88. Knežević, Z.; Mojović, L.; Adnađević, B. Immobilization of lipase on a hydrophobic zeolite type Y. *J. Serb. Chem. Soc.* **1998**, *63*, 257–264.
89. Palomo, J.M.; Fuentes, M.; Fernández-Lorente, G.; Mateo, C.; Guisan, J.M.; Fernández-Lafuente, R. General Trend of Lipase to Self-Assemble Giving Bimolecular Aggregates Greatly Modifies the Enzyme Functionality. *Biomacromolecules* **2003**, *4*, 1–6. [CrossRef] [PubMed]
90. Palomo, J.M.; Muñoz, G.; Fernández-Lorente, G.; Mateo, C.; Fernández-Lafuente, R.; Guisán, J.M. Interfacial adsorption of lipases on very hydrophobic support (octadecyl–Sepabeads): Immobilization, hyperactivation and stabilization of the open form of lipases. *J. Mol. Catal. B Enzym.* **2002**, *19–20*, 279–286. [CrossRef]
91. Fernandez-Lorente, G.; Rocha-Martín, J.; Guisán, J.M. Immobilization of Lipases by Adsorption on Hydrophobic Supports: Modulation of Enzyme Properties in Biotransformations in Anhydrous Media. *Methods Mol. Biol.* **2020**, *2100*, 143–158.
92. Serra, E.; Mayoral, Á.; Sakamoto, Y.; Blanco, R.M.; Díaz, I. Immobilization of lipase in ordered mesoporous materials: Effect of textural and structural parameters. *Microporous Mesoporous Mater.* **2008**, *114*, 201–213. [CrossRef]
93. Carteret, C.; Jacoby, J.; Blin, J. Using factorial experimental design to optimize biocatalytic biodiesel production from Mucor Miehei Lipase immobilized onto ordered mesoporous materials. *Microporous Mesoporous Mater.* **2018**, *268*, 39–45. [CrossRef]
94. Katiyar, M.; Abida, K.; Ali, A. Candida rugosa lipase immobilization over SBA-15 to prepare solid biocatalyst for cotton seed oil transesterification. *Mater. Today Proc.* **2021**, *36*, 763–768. [CrossRef]
95. Jacoby, J.; Pasc, A.; Carteret, C.; Dupire, F.; Stébé, M.; Coupard, V.; Blin, J.-L. Ordered mesoporous materials containing Mucor Miehei Lipase as biocatalyst for transesterification reaction. *Process. Biochem.* **2013**, *48*, 831–837. [CrossRef]
96. Kalantari, M.; Yu, M.; Yang, Y.; Strounina, E.; Gu, Z.; Huang, X.; Zhang, J.; Song, H.; Yu, C. Tailoring mesoporous-silica nanoparticles for robust immobilization of lipase and biocatalysis. *Nano Res.* **2017**, *10*, 605–617. [CrossRef]
97. Kalantari, M.; Yu, M.; Liu, Y.; Huang, X.; Yu, C. Engineering mesoporous silica microspheres as hyper-activation supports for continuous enzymatic biodiesel production. *Mater. Chem. Front.* **2019**, *3*, 1816–1822. [CrossRef]
98. Deon, M.; Ricardi, N.C.; De Andrade, R.C.; Hertz, P.F.; Nicolodi, S.; Costa, T.M.H.; Bussamara, R.; Benvenuti, E.V.; De Menezes, E.W. Designing a Support for Lipase Immobilization Based On Magnetic, Hydrophobic, and Mesoporous Silica. *Langmuir* **2020**, *36*, 10147–10155. [CrossRef] [PubMed]

99. Lisboa, M.C.; Rodrigues, C.A.; Barbosa, A.S.; Mattedi, S.; Freitas, L.S.; Mendes, A.A.; Dariva, C.; Franceschi, E.; Lima, Á.S.; Soares, C.M.F. New perspectives on the modification of silica aerogel particles with ionic liquid used in lipase immobilization with platform in ethyl esters production. *Process Biochem.* **2018**, *75*, 157–165. [[CrossRef](#)]
100. Virgen-Ortiz, J.J.; Pedrero, S.G.; Fernandez-Lopez, L.; Lopez-Carrobles, N.; Gorines, B.C.; Otero, C.; Fernandez-Lafuente, R. Desorption of Lipases Immobilized on Octyl-Agarose Beads and Coated with Ionic Polymers after Thermal Inactivation. Stronger Adsorption of Polymers/Unfolded Protein Composites. *Molecules* **2017**, *22*, 91. [[CrossRef](#)]
101. Garcia-Galan, C.; Berenguer-Murcia, Á.; Fernandez-Lafuente, R.; Rodrigues, R.C. Potential of Different Enzyme Immobilization Strategies to Improve Enzyme Performance. *Adv. Synth. Catal.* **2011**, *353*, 2885–2904. [[CrossRef](#)]
102. Barbosa, O.; Ortiz, C.; Berenguer-Murcia, Á.; Torres, R.; Rodrigues, R.C.; Fernandez-Lafuente, R. Glutaraldehyde in bio-catalysts design: A useful crosslinker and a versatile tool in enzyme immobilization. *RSC Adv.* **2014**, *4*, 1583–1600. [[CrossRef](#)]
103. Jin, W.; Xu, Y.; Yu, X.-W. Preparation of lipase cross-linked enzyme aggregates in octyl-modified mesocellular foams. *Int. J. Biol. Macromol.* **2019**, *130*, 342–347. [[CrossRef](#)]
104. Bi, Y.; Yu, M.; Zhou, H.; Zhou, H.; Wei, P. Biosynthesis of oleyl oleate in solvent-free system by *Candida rugosa* Lipase (CRL) immobilized in macroporous resin with cross-linking of aldehyde-dextran. *J. Mol. Catal. B Enzym.* **2016**, *133*, 1–5. [[CrossRef](#)]
105. Sandoval, G.; Marty, A. Screening methods for synthetic activity of lipases. *Enzym. Microb. Technol.* **2007**, *40*, 390–393. [[CrossRef](#)]
106. Liu, J.; Peng, J.; Shen, S.; Jin, Q.; Li, C.; Yang, Q. Enzyme entrapped in polymer-modified nanopores: The effects of macromolecular crowding and surface hydrophobicity. *Chemistry* **2013**, *19*, 2711–2719. [[CrossRef](#)]
107. Jin, W.; Xu, Y.; Yu, X.-W. Email Formation lipase cross-linked enzyme aggregates on octyl-modified mesocellular foams with oxidized sodium alginate. *Colloids Surf. B Biointerfaces* **2019**, *184*, 110501. [[CrossRef](#)] [[PubMed](#)]
108. Malar, C.G.; Seenuvasan, M.; Kumar, K.S.; Kumar, A.; Parthiban, R. Review on surface modification of nanocarriers to overcome diffusion limitations: An enzyme immobilization aspect. *Biochem. Eng. J.* **2020**, *158*, 107574. [[CrossRef](#)]
109. Jiang, Y.; Zheng, P.; Zhou, L.; Kong, W.; Gao, J.; Wang, J.; Gu, J.; Zhang, X.; Wang, X. Immobilization of lipase in hierarchically ordered macroporous/mesoporous silica with improved catalytic performance. *J. Mol. Catal. B Enzym.* **2016**, *130*, 96–103. [[CrossRef](#)]
110. Pang, J.; Zhou, G.; Liu, R.; Li, T. Esterification of oleic acid with methanol by immobilized lipase on wrinkled silica nanoparticles with highly ordered, radially oriented mesochannels. *Mater. Sci. Eng. C* **2016**, *59*, 35–42. [[CrossRef](#)]
111. Jiang, Y.; Sun, W.; Zhou, L.; Ma, L.; He, Y.; Gao, J. Improved Performance of Lipase Immobilized on Tannic Acid-Templated Mesoporous Silica Nanoparticles. *Appl. Biochem. Biotechnol.* **2016**, *179*, 1155–1169. [[CrossRef](#)]
112. Xiang, X.; Ding, S.; Suo, H.; Xu, C.; Gao, Z.; Hu, Y. Fabrication of chitosan-mesoporous silica SBA-15 nanocomposites via functional ionic liquid as the bridging agent for PPL immobilization. *Carbohydr. Polym.* **2018**, *182*, 245–253. [[CrossRef](#)]
113. Babaki, M.; Yousefi, M.; Habibi, Z.; Mohammadi, M.; Yousefi, P.; Mohammadi, J.; Brask, J. Enzymatic production of biodiesel using lipases immobilized on silica nanoparticles as highly reusable biocatalysts: Effect of water, t-butanol and blue silica gel contents. *Renew. Energy* **2016**, *91*, 196–206. [[CrossRef](#)]
114. Siódmiak, T.; Ziegler-Borowska, M.; Marszał, M.P. Lipase-immobilized magnetic chitosan nanoparticles for kinetic resolution of (R,S)-ibuprofen. *J. Mol. Catal. B Enzym.* **2013**, *94*, 7–14. [[CrossRef](#)]
115. Wang, P. Nanoscale biocatalyst systems. *Curr. Opin. Biotechnol.* **2006**, *17*, 574–579. [[CrossRef](#)] [[PubMed](#)]
116. Mehraabi, M.R.; Mohammadi, J.; Peyda, M.; Mohammadi, M. Covalent immobilization of *Candida antarctica* lipase on core-shell magnetic nanoparticles for production of biodiesel from waste cooking oil. *Renew. Energy* **2017**, *101*, 593–602. [[CrossRef](#)]
117. Ali, Z.; Tian, L.; Zhang, B.; Ali, N.; Khan, M.; Zhang, Q. Synthesis of fibrous and non-fibrous mesoporous silica magnetic yolk-shell microspheres as recyclable supports for immobilization of *Candida rugosa* lipase. *Enzym. Microb. Technol.* **2017**, *103*, 42–52. [[CrossRef](#)]
118. Ali, Z.; Tian, L.; Zhang, B.; Ali, N.; Zhang, Q. Synthesis of paramagnetic dendritic silica nanomaterials with fibrous pore structure (Fe<sub>3</sub>O<sub>4</sub>@KCC-1) and their application in immobilization of lipase from *Candida rugosa* with enhanced catalytic activity and stability. *N. J. Chem.* **2017**, *41*, 8222–8231. [[CrossRef](#)]
119. Esmi, F.; Nematian, T.; Salehi, Z.; Khodadadi, A.A.; Dalai, A.K. Amine and aldehyde functionalized mesoporous silica on magnetic nanoparticles for enhanced lipase immobilization, biodiesel production, and facile separation. *Fuel* **2021**, *291*, 120126. [[CrossRef](#)]
120. Khoobakht, G.; Kheiralipour, K.; Yuan, W.; Seifi, M.R.; Karimi, M. Desirability function approach for optimization of enzymatic transesterification catalyzed by lipase immobilized on mesoporous magnetic nanoparticles. *Renew. Energy* **2020**, *158*, 253–262. [[CrossRef](#)]
121. Shao, Y.B.; Jing, T.; Tian, J.Z.; Zheng, Y.J.; Shang, M.H. Characterization and optimization of mesoporous magnetic nanoparticles for immobilization and enhanced performance of porcine pancreatic lipase. *Chem. Pap.* **2015**, *69*, 1298–1311. [[CrossRef](#)]
122. Khoobi, M.; Motevalizadeh, S.F.; Asadgol, Z.; Forootanfar, H.; Shafiee, A.; Faramarzi, M.A. Synthesis of functionalized poly-ethylenimine-grafted mesoporous silica spheres and the effect of side arms on lipase immobilization and application. *Biochem. Eng. J.* **2014**, *88*, 131–141. [[CrossRef](#)]
123. Ye, P.; Jiang, J.; Xu, Z.-K. Adsorption and activity of lipase from *Candida rugosa* on the chitosan-modified poly(acrylonitrile-co-maleic acid) membrane surface. *Colloids Surf. B Biointerfaces* **2007**, *60*, 62–67. [[CrossRef](#)]

124. Carvalho, N.B.; Vidal, B.T.; Barbosa, A.S.; Pereira, M.M.; Mattedi, S.; Freitas, L.D.S.; Lima, Á.S.; Soares, C.M. Lipase immobilization on silica xerogel treated with protic ionic liquid and its application in biodiesel production from different oils. *Int. J. Mol. Sci.* **2018**, *19*, 1829. [[CrossRef](#)]
125. Katiyar, M.; Ali, A. One-pot lipase entrapment within silica particles to prepare a stable and reusable biocatalyst for transesterification. *J. Am. Oil Chem. Soc.* **2015**, *92*, 623–632. [[CrossRef](#)]
126. Ficanha, A.M.M.; Antunes, A.; Oro, C.E.D.; Dallago, R.M.; Mignoni, M.L. Immobilization of candida antarctica b (calb) in silica aerogel: Morphological characteristics and stability. *Biointerfaces Res. Appl. Chem.* **2020**, *10*, 6744–6756.
127. Cazaban, D.; Illanes, A.; Wilson, L.; Betancor, L. Bio-inspired silica lipase nanobiocatalysts for the synthesis of fatty acid methyl esters. *Process. Biochem.* **2018**, *74*, 86–93. [[CrossRef](#)]